

Short time-scale variability of γ -ray-emitting narrow-line Seyfert 1 galaxies in optical and UV bands

F. D’Ammando^{1*}

¹INAF – Istituto di Radioastronomia, Via Gobetti 101, I-40129 Bologna, Italy

Accepted. Received; in original form

ABSTRACT

We report the first systematic analysis of single exposures of all optical and ultraviolet (UV) observations performed by the UltraViolet and Optical Telescope (UVOT) on board the *Neil Gehrels Swift Observatory* satellite available up to 2019 April of six γ -ray-emitting narrow-line Seyfert 1 galaxies (NLSy1). Rapid variability has been significantly detected on hours time-scale for 1H 0323+342, SBS 0846+513, PMN J0948+0022, and PKS 2004–447 in 18 observations for a total of 34 events. In particular, we report the first detection of significant variability on short time-scale (3–6 ks) in optical for PKS 2004–447, and UV for 1H 0323+342 and PMN J0948+0022. The shortest variability time-scale observed for 1H 0323+342, SBS 0846+513, PMN J0948+0022, and PKS 2004–447 (assuming a Doppler factor $\delta = 10$) gives a lower limit on the size of emission region between 9.7×10^{14} (for SBS 0846+513) and 1.6×10^{15} cm (for 1H 0323+342), suggesting that the optical and UV emission during these events is produced in compact regions within the jet. These observations provide unambiguous evidence about the relativistically beamed synchrotron emission in these sources, similar to blazars. A remarkable variability has been observed for PMN J0948+0022 on 2009 June 23 with an increase from ~ 1.1 to 0.4 mag going from v to $w2$ filter in ~ 1.6 h and a decrease at the initial level in a comparable time. The higher fractional flux change observed for this and other events at lower frequencies suggests that the synchrotron emission is more contaminated by thermal emission from accretion disc at higher frequencies.

Key words: radiation mechanisms: non-thermal – galaxies: active – galaxies: jets – galaxies: Seyfert – ultraviolet: galaxies

1 INTRODUCTION

Narrow-line Seyfert 1 galaxies (NLSy1) are a class of active galactic nuclei (AGN) characterized by peculiar optical characteristics, that is, full width at half-maximum of the $H\beta$ broad emission line $< 2000 \text{ km s}^{-1}$, the flux ratio of $[O \text{ III}]$ to $H\beta < 3$, and a strong Fe_{II} bump (see e.g. Pogge 2000, for a review). Only a small fraction of NLSy1 are radio loud ($< 7\%$, Komossa et al. 2006; Zhou et al. 2006; Rakshit et al. 2017), a fraction lower than that estimated for quasars and broad-line AGN (15–20 per cent, e.g., Jiang et al. 2007; Kellermann et al. 2016). Observations with the Large Area Telescope (LAT) on board the *Fermi Gamma-ray Space Telescope* have revealed NLSy1 as a new class of γ -ray-emitting AGN with blazar-like properties (Abdo et al. 2009; D’Ammando et al. 2012, 2015a; Ajello et al. 2020). It is a

very small class of objects up to now. Nine NLSy1¹ are included in the Fourth *Fermi* LAT source catalogue (4FGL; Abdollahi et al. 2020), even considering the Data Release 2 of the 4FGL catalogue², which covers 10 yr (i.e., 2008 August 4–2018 August 4) of LAT data. Past studies have suggested that NLSy1 are powered by high-accretion processes (e.g., Peterson et al. 2000; Grupe 2004), therefore investigating the properties of these sources is of interest for understanding similarities and differences with the other γ -ray-emitting AGN. Compared to the population of blazars, which includes BL Lacs and flat spectrum radio quasars (FSRQ), NLSy1 seems to share properties similar to FSRQ, but with typically lower γ -ray luminosities (e.g.,

¹ New deep spectroscopic observations of TXS 2116–077 dis-favour its classification as an NLSy1 (Järvelä et al. 2020).

² https://fermi.gsfc.nasa.gov/ssc/data/access/lat/10yr_catalog/

* E-mail: dammando@ira.inaf.it

Foschini et al. 2015; D’Ammando et al. 2016; D’Ammando 2019).

In D’Ammando (2020), we have analysed the optical, ultraviolet (UV), and X-ray observations performed by the *Neil Gehrels Swift Observatory* during 2006 July–2019 April of six γ -ray-emitting NLSy1 (i.e., 1H 0323+342, SBS 0846+513, PMN J0948+0022, PKS 1502+036, FBQS J1644+2619, and PKS 2004–447) to investigate their flux variability and spectral changes. A significant flux change has been observed in the optical and UV bands on time-scale of one day for 1H 0323+342 and a few days for SBS 0846+513, PMN J0948+0022, and PKS 1502+036, clearly related to an increase of the non-thermal emission from a relativistic jet. On a long-term scale, a large variability amplitude has been observed for all six γ -ray-emitting NLSy1, significantly higher than the variability observed in other radio-loud NLSy1 not detected in γ -rays. These results have confirmed the dominance of the jet emission in the optical and UV part of their spectrum.

Intraday optical variability has been investigated in the past and detected in 1H 0323+342 (Itoh et al. 2014; Ojha et al. 2019), SBS 0846+513 (Maune et al. 2014; Paliya & Stalin 2016), and PMN J0948+0022 (Liu et al. 2010; Itoh et al. 2013; Maune et al. 2013), with variations higher than 0.3 mag within a few hours, while no optical intraday variability has been detected in PKS 1502+036 (Ojha et al. 2019). Variability amplitude of few per cent (4–16 per cent) on time-scales of 3–5 h has been reported by Ojha et al. (2020) for 1H 0323+342, PMN J0948+0022, and FBQS J1644+2619.

Here, we present a systematic analysis on short time-scale of all optical and UV observations performed by the UltraViolet and Optical Telescope (UVOT; Roming et al. 2005) on board *Swift* for the six γ -ray-emitting NLSy1 studied in D’Ammando (2020) in the same period (i.e. 2006 July–2019 April). The paper is organized as it follows. Section 2 describes the *Swift*–UVOT observations and data analysis. Optical and UV variability results are reported and discussed in Section 3, while in Section 4 we summarize our results.

2 *SWIFT*–UVOT OBSERVATIONS AND DATA ANALYSIS

The *Neil Gehrels Swift Observatory* satellite (Gehrels et al. 2004) observed the γ -ray-emitting NLSy1 1H 0323+342, SBS 0846+513, PMN J0948+0022, PKS 1502+036, FBQS J1644+2619, and PKS 2004–447 for 136, 32, 45, 16, 11, and 32 epochs, respectively, up to 2019 April. The results of the analysis of X-Ray Telescope observations have been presented in D’Ammando (2020). In this work, we focus on UVOT observations. In particular, we analyze the data corresponding to observations with multiple exposures with the same filter at the same epoch searching for variability on subdaily time-scales. Table 1 reports the number of observations with multiple exposures of the six sources studied here separated for each filter, and the total number considering all filters together. In Appendix A, we report the results of the analysis of the images obtained by summing the multiple exposures with the same filter at the same epoch.

During the *Swift* pointings, the UVOT instrument observed the sources in its optical (*v*, *b*, and *u*) and UV (*w1*, *m2*, and *w2*) photometric bands (Poole et al. 2008; Breeveld et al. 2010). UVOT data in all filters were analysed with the *uvotmaghist* task included in the HEASOFT package (v6.26.1) and the 20170922 CALDB-UVOTA release. Source counts were extracted from a circular region of 5 arcsec radius centred on the source, while background counts were derived from a circular region with 20 arcsec radius in a nearby source-free region. All UVOT exposures were checked for possible small scale sensitivity (‘sss’) problems, which occur when the source falls on small detector regions where the sensitivity is lower³. This issue has been observed in 28 of the 286 epochs analysed and only in the UV filters, as expected because the bad areas cover ~ 7 per cent of the central 5×5 arcmin square of the field of view in UV filters, while ~ 0.7 per cent of the central area in optical filters is affected. Exposures affected by the ‘sss’ issue have been excluded in the following analysis.

After having analysed each single exposure, we have searched for significant ($> 3\sigma$) changes of magnitude between two consecutive exposures collected with the same filter at the same epoch. The significance is calculated as $\Delta\text{mag}/\sqrt{(\sigma_1^2 + \sigma_2^2)}$, where $\Delta\text{mag} = |\text{mag}_1 - \text{mag}_2|$, mag_1 and mag_2 are the magnitude of the two exposures, and σ_1 and σ_2 are the corresponding uncertainties. Systematic errors due to uncertainties in the photometric zero points are included in the total uncertainties considered. In Table 2, we report for each event the date and filter, magnitude, and significance of detection for the single exposure, Δmag , significance of change between the two exposures, and the time elapsed between the two exposures.

3 RESULTS AND DISCUSSION

Significant variability has been observed on hours time-scale for 1H 0323+342, SBS 0846+513, PMN J0948+0022, and PKS 2004–447 in 18 observations for a total of 34 events taken into account each filter separately. In particular, a change of magnitude has been detected in eight observations for 1H 0323+342 (for a total of 13 events considering the different filters), in one observation for SBS 0846+513 (for a total of 2 events considering the different filters), in eight observations for PMN J0948+0022 (for a total of 18 events considering the different filters), and in one observation for PKS 2004–447 (for a total of 1 event considering the different filters). In 4 of the 18 observations (on 2010 November 10 and 2015 November 26 for 1H 0323+342; on 2009 May 5 for PMN J0948+0022; on 2013 November 20 for PKS 2004–447) we have seen a decrease of the activity between the two exposures on a time-scale of ~ 6 ks. In those cases, the lack of observations before the tentative peak of activity leaves open the possibility of a more rapid rising time with respect to the decreasing part of the activity observed by *Swift*. In case of FBQS J1644+2619, a change of 0.474 mag has been observed on 2015 April 9 in the *m2* filter, but at a significance of 2.2σ . No changes at a significance $> 2\sigma$ has been observed for PKS 1502+036.

³ https://swift.gsfc.nasa.gov/analysis/uvot_digest/sss_check.html

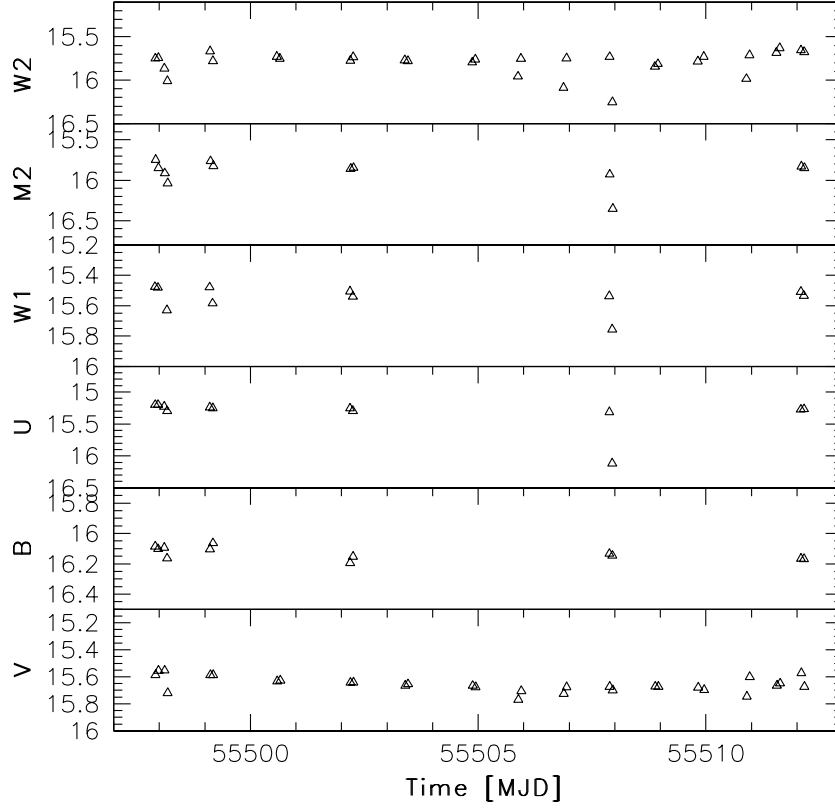


Figure 1. Light curve of 1H 0323+342 in the six UVOT filters for the period 2010 October 28 (MJD 55497)–November 13 (MJD 55513) considering single exposures. Errors are small (0.04–0.06 mag), therefore are not shown in the plot.

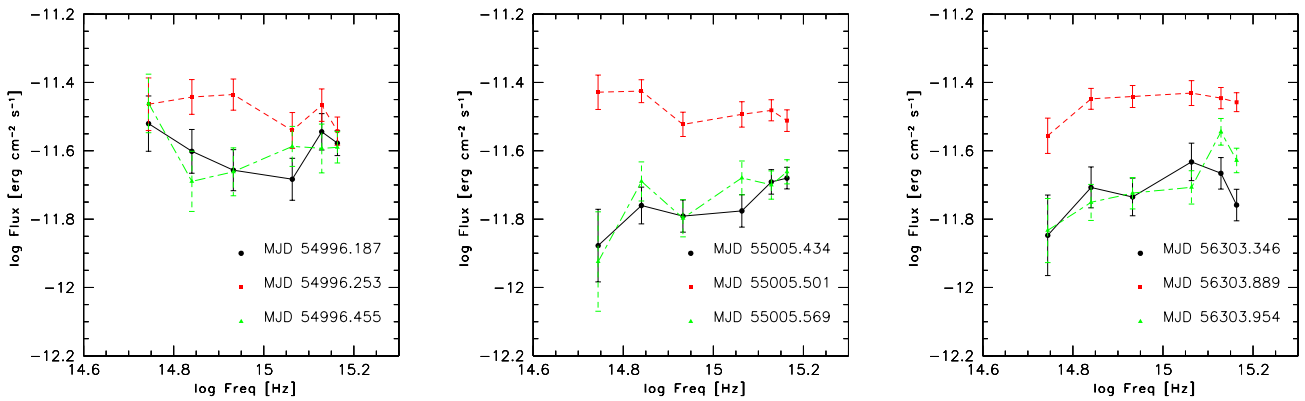


Figure 2. SED of PMN J0948+0022 obtained by *Swift*–UVOT from *v* to *w2* filters on 2009 June 14 (MJD 54996; left-hand panel), 2009 June 23 (MJD 55005; centre panel), and 2013 January 11 (MJD 56003; right-hand panel). Fluxes are corrected for Galactic extinction. Different symbols and colours refer to images collected at different times within the same *Swift* observation.

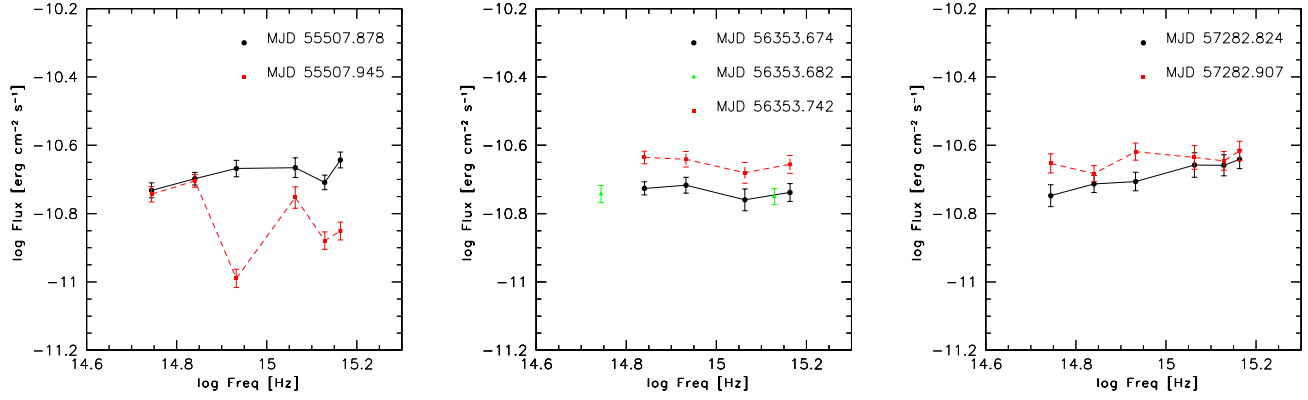


Figure 3. SED of 1H 0323+323 obtained by *Swift*-UVOT from *v* to *w2* filters on 2009 June 25 (MJD 55507; left-hand panel) and 2013 March 2 (MJD 56353; centre panel), and 2015 July 17 (MJD 57282; right-hand panel). Fluxes are correct for Galactic extinction. Different symbols and colours refer to images collected at different times within the same *Swift* observation.

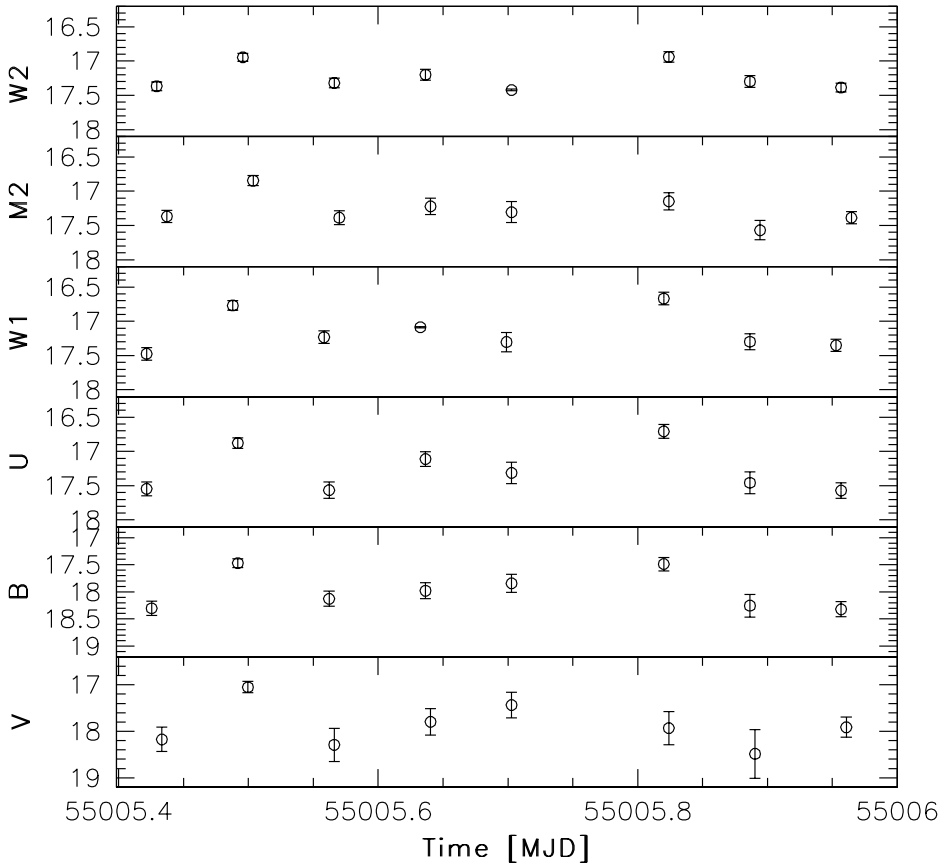
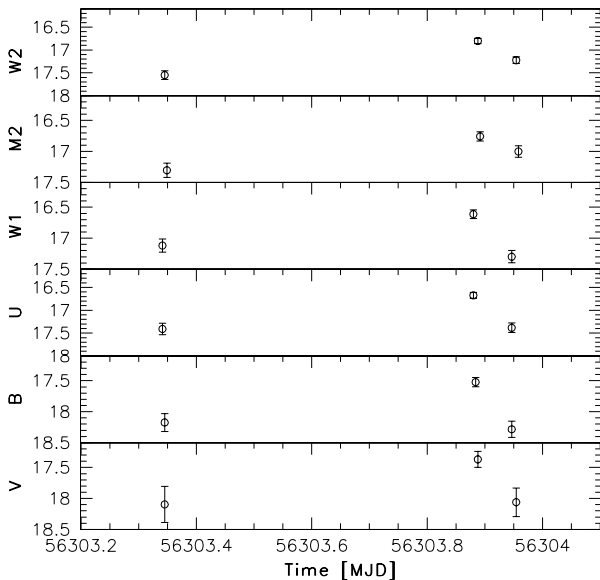


Figure 4. Light curve of the single exposures of PMN J0948+0022 in the six UVOT filters collected on 2009 June 23 (MJD 55005).

Table 1. The number of *Swift*–UVOT observations with multiple exposures in the same epoch in each UVOT filter for the six sources studied, and total number of events studied. Redshift of each source and central wavelength of each filter are reported.

Source name	z	v (5468 Å)	b (4392 Å)	u (3465 Å)	$w1$ (2600 Å)	$m2$ (2246 Å)	$w2$ (1928 Å)	Total events
1H 0323+342	0.061	86	76	80	79	70	97	488
SBS 0846+513	0.584	20	22	23	27	22	22	136
PMN J0948+0022	0.585	23	23	42	24	23	23	158
PKS 1502+036	0.408	3	3	6	6	4	8	30
FBQS J1644+2619	0.145	4	4	6	6	5	5	30
PKS 2004–447	0.240	5	5	11	11	13	10	55

**Figure 5.** Light curve of the single exposures of PMN J0948+0022 in the six UVOT filters collected on 2013 January 11 (MJD 56303).

Careful checks made for each single image ensure that these events are not related to instrumental artifacts. Three factors can influence the detection of such a rapid change of magnitude with UVOT: the number of observations with multiple images collected at the same epoch, the average brightness of the source, and its activity state in the period studied.

The number of observations with multiple exposures in optical and UV filters is comparable (442 observations summing v , b , and u filters, 455 observations summing $w1$, $m2$, and $w2$ filters), although due to the ‘sss’ issue some events in the UV filters have been discarded. This reflects in a comparable number of events in optical (19 events, 14 of them observed in u) and UV (15 events, 8 of them observed in $w2$) filters. Considering each object separately, we notice that for PKS 1502+036, FBQS J1644+2644, and PKS 2004–447, the number of observations with multiple exposures is relatively low (30, 30, and 55, respectively; see Table 1), while it is significantly higher for 1H 0323+342,

SBS 0846+513, and PMN J0948+0022 (488, 136, and 158, respectively; see Table 1). However, the percentage of events detected for the latter three sources is quite different: ~ 3 per cent, ~ 1.5 per cent, and ~ 12 per cent, respectively. This suggests that the average brightness of the source, and thus the uncertainties obtained, can play an important role in revealing variability on short-term time-scales. Considering the analysis of the images obtained by summing the single exposures collected at each epoch (see Table A1–A6 in Appendix A) the median of the uncertainties are: 0.06 mag for 1H 0323+342, 0.08 mag for PMN J0948+0022, 0.10 mag for FBQS J1644+2619, 0.19 mag for PKS 1502+036, 0.22 mag for PKS 2004–447, and 0.24 mag for SBS 0846+513. Uncertainties are even larger when considering the single images instead of the summed images. This can explain the low number of events observed for SBS 0846+513. In this context, we would have expected a larger number of events for 1H 0323+342. However, the smaller percentage of events, if compared to PMN J0948+0022, may be due to the very low long-term variability amplitude observed for this source over the entire *Swift* monitoring (see Table A8 in Appendix A).

In Table 3, we report the short-term variability amplitude of these rapid events calculated as the ratio between the peak magnitude observed in each epoch and the average magnitude estimated over the entire period. Differently from what observed for SBS 0846+513, PMN J0948+0022, and PKS 2004–447, in case of 1H 0323+342 the short-term variability amplitude is quite low for each event. It is worth mentioning that only for two events (on MJD 55507 in $m2$ filter for 1H 0323+342, and on MJD 56012 in u filter for PMN J0948+0022) the source has been observed with a lower magnitude with respect to average value obtained over the entire *Swift* monitoring, confirming that almost all the short time-scale variability events are detected during high activity states.

The magnitude changes observed in the different filters (considering all the four sources in Table 2) vary in the interval: 0.42–1.12 in v , 0.23–0.83 in b , 0.19–0.80 in u , 0.22–0.70 in $w1$, 0.42–0.55 in $m2$, and 0.21–0.75 in $w2$, with a higher amplitude of variability in the optical bands with respect to the UV ones. This is opposite to the behaviour usually observed in quasars, that is, increasing variability with increasing frequencies (e.g., Vanden Berk et al. 2004), in agreement with a dominant contribution of the synchrotron emission in both optical and UV bands in these NLSy1. However, in this context, the larger changes observed in optical with respect to UV may be related also to the presence, in addition to variable emission from a jet, of an almost constant emission

Table 2. Results of the search for significant change of magnitude in consecutive UVOT exposures in the same epoch with the same filter for the six γ -ray-emitting NLSy1.

Source name	Date		Filter	Single exposures		Δmag	Change of magnitude	
	Gregorian	MJD		Mag	Significance _{image} (σ)		Significance _{change} (σ)	ΔT (s)
1H 0323+342	2010-11-05	55505	<i>w2</i>	15.958 ± 0.043	48.9			
				15.753 ± 0.042	56.2	0.205	3.4	5786
	2010-11-06	55506	<i>w2</i>	16.085 ± 0.043	47.8			
				15.748 ± 0.042	56.3	0.337	5.6	5700
	2010-11-07	55507	<i>u</i>	15.312 ± 0.042	40.9			
				16.118 ± 0.054	25.5	0.804	11.8	5798
			<i>w1</i>	15.537 ± 0.049	34.5			
				15.755 ± 0.053	29.5	0.218	3.0	5812
			<i>m2</i>	15.929 ± 0.056	26.4			
				16.352 ± 0.065	20.4	0.423	4.9	5716
			<i>w2</i>	15.732 ± 0.045	43.2			
				16.252 ± 0.050	32.0	0.520	7.7	5762
	2010-11-10	55510	<i>w2</i>	15.984 ± 0.043	51.2			
				15.710 ± 0.042	53.9	0.274	4.6	5973
	2010-11-28	55528	<i>w2</i>	15.930 ± 0.047	37.6			
				15.554 ± 0.043	48.4	0.376	5.9	17345
	2013-03-02	56353	<i>b</i>	16.205 ± 0.047	31.2			
				15.974 ± 0.044	34.0	0.231	3.5	5778
			<i>u</i>	15.437 ± 0.046	33.7			
				15.244 ± 0.045	33.6	0.193	3.0	5789
			<i>w2</i>	15.971 ± 0.048	34.8			
				15.764 ± 0.049	32.3	0.207	3.0	5713
		2015-09-17	<i>u</i>	15.409 ± 0.053	25.2			
				15.187 ± 0.050	29.2	0.222	3.0	7154
	2015-11-26	57352	<i>u</i>	15.221 ± 0.042	40.4			
				15.454 ± 0.054	26.1	0.234	3.4	6568
SBS 0846+513	2013-04-22	56404	<i>v</i>	16.388 ± 0.049	26.2			
				15.972 ± 0.040	36.5	0.416	6.6	5143
			<i>u</i>	16.517 ± 0.053	25.7			
				16.265 ± 0.054	25.2	0.252	3.3	5118
PMN J0948+0022	2009-05-05	54956	<i>u</i>	16.542 ± 0.073	16.9			
				16.914 ± 0.091	12.9	0.372	3.2	5768
	2009-06-14	54996	<i>u</i>	17.212 ± 0.136	8.3			
				16.660 ± 0.099	11.8	0.552	3.3	5760
	2009-06-23	55005	<i>v</i>	18.174 ± 0.262	4.2			
				17.051 ± 0.122	9.2	1.123	3.9	5807
			<i>b</i>	18.303 ± 0.132	8.5			
				17.469 ± 0.081	14.6	0.834	5.4	5907
			<i>u</i>	17.545 ± 0.103	11.2			
				16.878 ± 0.076	16.0	0.667	5.2	5928
			<i>w1</i>	17.474 ± 0.090	13.2			
				16.770 ± 0.070	18.2	0.704	6.6	5979
			<i>m2</i>	17.367 ± 0.089	13.5			
				16.844 ± 0.076	16.5	0.523	4.5	5778
			<i>w2</i>	17.366 ± 0.064	21.0			
				16.947 ± 0.059	23.8	0.419	4.8	5857

from an accretion disc at higher frequencies, as usually observed in FSRQ (e.g. D’Ammando et al. 2011; Raiteri et al. 2012).

For 1H 0323+342 and PMN J0948+0022, changes of magnitude have been significantly detected in both optical and UV bands, at least one time for all six filters, except for the *v* filter in case of 1H 0323+342 (see Fig. 1). On the other hand, for SBS 0846+513 and PKS 2004–447 significant variability has been observed only in optical bands. Considering that in the latter two sources a prominent ac-

cretion disc is missing (see e.g. D’Ammando et al. 2013; Orienti et al. 2015), the lack of variability on hours time-scale in UV should not be related to the presence of thermal emission from accretion disc that can dilute the jet emission. For PKS 1502+036 and FBQS J1644+2619, the lack of variability on hours time-scale can be mainly related to the small number of *Swift*–UVOT observations with multiple exposures available at the same epoch. Moreover, in case of PKS 1502+036, the source is relatively faint (see the average magnitude in Table A7 in Appendix A), therefore the large

Table 2. Results of the search for significant change of magnitude in consecutive UVOT exposures in the same epoch with the same filter for the six γ -ray-emitting NLSy1. Note: The asterisk * indicates that multiple exposures are present only for the filters reported in table.

Source name	Date		Filter	Single exposures		Change of magnitude		
	Gregorian	MJD		Mag	Significance _{image} (σ)	Δ mag	Significance _{change} (σ)	Δ T (s)
PMN J0948+0022	2012-03-26	56012*	<i>u</i>	17.778 \pm 0.047	30.8			
				17.523 \pm 0.043	37.3	0.255	4.0	17275
	2012-03-30	56016*	<i>u</i>	17.219 \pm 0.039	46.3			
				16.998 \pm 0.037	52.4	0.221	4.1	5757
	2012-04-23	56040*	<i>u</i>	17.404 \pm 0.056	23.7			
				16.873 \pm 0.068	18.4	0.531	6.0	30340
	2012-12-30	56291*	<i>u</i>	16.196 \pm 0.097	12.3			
				15.703 \pm 0.067	19.1	0.494	4.2	5265
			<i>w1</i>	16.344 \pm 0.057	25.3			
				15.721 \pm 0.072	17.8	0.623	6.8	5361
	2013-01-11	56303	<i>b</i>	18.175 \pm 0.146	7.7			
				17.524 \pm 0.074	16.3	0.651	4.0	46709
			<i>u</i>	17.411 \pm 0.126	9.0			
				16.672 \pm 0.065	19.2	0.739	5.2	46658
			<i>w1</i>	17.120 \pm 0.108	10.8			
				16.613 \pm 0.068	19.3	0.507	4.0	46583
			<i>m2</i>	17.304 \pm 0.113	10.2			
				16.756 \pm 0.075	16.8	0.548	4.0	47042
			<i>w2</i>	17.549 \pm 0.097	12.2			
				16.800 \pm 0.058	24.4	0.749	6.6	46833
PKS 2004-447	2013-11-20	56616*	<i>u</i>	18.310 \pm 0.062	20.4			
				18.665 \pm 0.076	15.6	0.356	3.6	5820

uncertainties obtained due to the short observation time of the single exposures prevent us to detect significant changes of magnitude. In case of FBQS J1644+2619, the long-term variability amplitude estimated over all *Swift* observations available is low (< 2) in all filters (see Table A8 in Appendix A), indicating a period of relatively low activity of the source during the *Swift* monitoring.

In Table 3, we report the fractional flux change obtained for the 34 events identified in the UVOT data.

For PMN J0948+0022, the fractional flux change is higher in the optical filters than in the UV ones. The spectral energy distribution (SED) of the source in optical and UV (from *v* to *w2* filter) is shown in Fig. 2 for three events with images in all filters, corresponding to MJD 54996 (left-hand panel), MJD 55005 (centre panel), and MJD 56303 (right-hand panel). The UVOT magnitudes are corrected for Galactic extinction using the $E(B - V)$ value from Schlafly & Finkbeiner (2011) and the extinction laws from Cardelli et al. (1989) and converted to flux densities using the conversion factors from Breeveld et al. (2010). The lower fractional flux change in UV can be related to the presence of a bright accretion disc with a luminosity of $L_{\text{disc}} = 5.7 \times 10^{45} \text{ erg s}^{-1}$ (D’Ammando et al. 2015b) peaking in the UV part of the spectrum that can partly dilute the jet emission reducing the variation of the emission. The presence of an accretion disc may be seen in the UV part of the three SED obtained before the short-term variability events (MJD 54996.187, 55005.434, 56303.346). A possible shift of the synchrotron peak to higher frequencies is observed at the time of the short-term variability events on MJD 54996.253 and MJD 56303.889. After the variability event, the optical and UV flux levels are comparable to those before the event. On

MJD 56303.954, a hint of the accretion disc seems to be present 1.6 h after the peak flux.

For 1H 0323+342, the behaviour observed during the short-term variability events may be consistent with jet emission that dominates in the optical and a significant contribution from the accretion disc in the UV. However, a more complicated behaviour seems to emerge in some events. A higher fractional flux change has been observed on MJD 55507 in the *u* filter with respect to the UV band, but no evidence of variability is detected in the *v* and *b* filters (Fig. 3, left-hand panel). Owing to the low redshift of the source ($z = 0.061$), the host galaxy may contribute to the total emission in optical bands. Therefore, the thermal emission from the host may dilute the variability amplitude in the *v* and partly *b* filters (see e.g., Ojha et al. 2020). On MJD 57282, a change of magnitude has been observed only in the optical band (in particular in *u* filter and at lower significance in the *v* filter; Fig 3, right-hand panel). On the contrary a comparable fractional flux change has been observed in optical (*b* and *u* filters) and UV (*w1* and *m2* filters) bands on MJD 56353 (Fig 3, centre panel)⁴. This chromatic behaviour is likely intrinsic, and is related to injection/acceleration of particles in the jet. No significant change of the overall shape of the optical-UV spectrum has been observed between the two exposures on MJD 57282 and MJD 56353.

Comparing PMN J0948+0022 and 1H 0323+342, a higher fractional flux change has been observed in the former (an average fractional flux change of 75 per cent) with

⁴ On MJD 56353 only one image has been collected in the *v* and *w2* filters.

Table 3. Fractional change of flux, rest-frame time-scale, and short-term variability amplitude based on significant change of magnitude in consecutive UVOT exposures in the same epoch with the same filter for the six γ -ray-emitting NLSy1 reported in Table 2. The short-term variability amplitude ($V_{\text{amp, ST}}$) is calculated as the ratio between the peak magnitude observed in each epoch and the average magnitude estimated over the entire period (see Table A8).

Source name	Date		Filter	Fractional Change %	ΔT_{rest} (s)	$V_{\text{amp, ST}}$
	Gregorian	MJD				
1H 0323+342	2010-11-05	55505	<i>w2</i>	21	5453	1.03
	2010-11-06	55506	<i>w2</i>	36	5372	1.03
	2010-11-07	55507	<i>u</i>	110	5465	1.03
			<i>w1</i>	22	5478	1.02
			<i>m2</i>	48	5387	0.96
			<i>w2</i>	61	5431	1.05
	2010-11-10	55510	<i>w2</i>	29	5630	1.07
	2010-11-28	55528	<i>w2</i>	41	16348	1.24
	2013-03-02	56353	<i>b</i>	24	5445	1.23
			<i>u</i>	19	5456	1.10
			<i>w2</i>	21	5385	1.02
	2015-09-17	57282	<i>u</i>	23	6743	1.16
	2015-11-26	57352	<i>u</i>	24	6190	1.12
	2013-04-22	56404	<i>v</i>	46	3247	11.89
			<i>u</i>	26	3231	14.29
SBS 0846+513						
PMN J0948+0022	2009-05-05	54956	<i>u</i>	41	3639	2.09
	2009-06-14	54996	<i>u</i>	66	3634	1.87
	2009-06-23	55005	<i>v</i>	181	3664	1.96
			<i>b</i>	116	3727	1.85
			<i>u</i>	85	3740	1.52
			<i>w1</i>	91	3772	1.41
			<i>m2</i>	62	3645	1.40
			<i>w2</i>	47	3695	1.28
	2012-03-26	56012	<i>u</i>	26	10899	0.82
	2012-03-30	56016	<i>u</i>	23	3632	1.36
	2012-04-23	56040	<i>u</i>	63	19142	1.53
	2012-12-30	56291	<i>u</i>	58	3322	4.63
			<i>w1</i>	78	3382	3.80
	2013-01-11	56303	<i>b</i>	82	29469	1.76
			<i>u</i>	98	29437	1.85
PKS 2004-447			<i>w1</i>	60	29390	1.63
			<i>m2</i>	66	29679	1.52
			<i>w2</i>	99	29548	1.48
	2013-11-20	56616	<i>u</i>	39	4127	1.87

respect to the latter (an average fractional flux change of 37 per cent), in agreement with the higher long-term variability amplitude observed in the different filters over the long-term monitoring provided by *Swift* (see Table A8 in Appendix A). Differently from the other γ -ray-emitting NLSy1, over a long time-scale the variability amplitude of 1H 0323+342 increases with increasing frequencies, and this may be related to a less powerful jet when the source is not in a high activity period, and a larger contribution of a quite bright accretion disc (1.4×10^{45} erg s $^{-1}$, Abdo et al. 2009). Moreover, as previously reported, a steady thermal emission from the host galaxy may contribute to the optical emission with a dilution of the optical synchrotron emission.

Notes on individual sources are reported below.

1H 0323+342: the source has been monitored on daily basis between 2010 October 28 and November 30 (see Fig. A1 in Appendix A), showing five variability events in *w2*, the best sampled filter, and in particular four events between 2010 November 5 and 10 (see Fig. 1). No significant events have been observed in *v* filter, where the number of

exposures is comparable to the *w2* filter. The lower variability observed in *v* filter (and more generally in the optical part of the spectrum, see the long-term variability amplitude in Table A8 in Appendix A) for 1H 0323+342 can be due to a higher contamination from thermal emission from the host galaxy. Moreover, in this source the accretion disc can contribute more significantly to the total emission in optical-UV. In the other filters only one event has been observed in 2010 November, but it can be due to a sparse sampling.

SBS 0846+513: notwithstanding the source has shown the largest long-term variability amplitude in the optical and UV bands during the *Swift* monitoring (see Table A8 in Appendix A), a change of magnitude has been significantly detected only in one observation. This is mainly due to the relatively large uncertainties on magnitude obtained for the single exposures related also to the relatively faintness of the source (see the average magnitudes in Table A7 of Appendix A). Moreover, in case of 2013 April 22, the exposures in *w1* and *w2* filters have been affected by the ‘sss’ issue not

allowing us to properly compare the variability in optical and UV bands. A few other events with a large change of magnitude but at a significance of $2 < \sigma < 3$ have been observed, with a Δmag of 0.606 (on 2013 January 30) and 0.974 (on 2019 March 20) in u filter, 0.893 (on 2019 January 16), 0.635 (on 2011 August 30), and 0.584 (on 2011 January 30) in $m2$ filter, 0.576 (on 2019 March 6) and 0.641 (on 2019 April 3) in $w2$ filter.

PMN J0948+0022: a spectacular variability has been observed on 2009 June 23 (see Fig. 4) with an increase from ~ 1.1 to 0.4 mag going from v to $w2$ filter in ~ 1.6 h (corresponding to 1 h in rest frame, see Table 3) and a decrease at the initial level in a comparable time (see also Fig. 2, centre panel). The approximate symmetry of the event, with a similar rising and decaying time, suggests that the relevant time-scale in this case can be the light crossing time of the emitting region (e.g. Chiaberge & Ghisellini 1999). A second peak with a smaller amplitude and at lower significance has been observed a few hours later. A similar rapid variability in optical bands has been reported for PMN J0948+0022 in Liu et al. (2010) and Eggen et al. (2013). The lower variability amplitude observed at higher frequencies implies that the synchrotron emission is more contaminated by thermal emission from accretion disc at higher frequency, as expected by the SED modelling of the source (see e.g. D’Ammando et al. 2015b). Another flaring event from this source on a longer time-scale is shown in Fig. 5 (left-hand panel), with a decreasing variability going to higher frequencies. In addition, several other events at a significance of $2 < \sigma < 3$ have been observed. In particular, on 2009 May 5 simultaneously to a significant change in u band, a Δmag of 0.430 and 0.427 in v and b filters has been observed with a significance of 2.5σ and 2.9σ , respectively. In the same way, on 2009 June 14, simultaneously to a significant change in u band, there is a Δmag of 0.724, 0.385, and 0.256 in b , $w1$, and $w2$ filters with a significance of 2.9σ , 2.5σ , and 2.1σ , respectively (see also Fig. 2, left-hand panel). Moreover, it is worth mentioning that on 2009 June 4, a Δmag of 0.869, 0.437, and 0.440 has been observed in v , b , and $w1$ filters with a significance of 2.4σ , 2.5σ , and 2.3σ , respectively. The higher number of events observed in u filter is related to the fact that 21 of the 45 *Swift*–UVOT observations are performed only in that filter.

PKS 2004–447: similarly to SBS 0846+513, the quite large uncertainties on the magnitudes estimated in single exposures, related to the relatively faintness of the source (see Table A7 in Appendix A) reduce the significance of the change of magnitude observed. A few other events with a large change of magnitude but at a significance of $2 < \sigma < 3$ have been observed, with a Δmag of 0.387 (on 2012 September 30) and 0.791 (on 2014 March 14) in $w1$ filter, and 0.712 (on 2013 October 20) and 0.854 (on 2016 May 1) in $w2$ filter.

Large amplitude variability events on short time-scales in radio-quiet NLSy1 are usually rare (e.g., Klimek et al. 2004), although not completely absent in literature, as shown by optical variations of 0.1–0.2 mag of IRAS 13224–3809 on time-scales of an hour (Miller et al. 2000). In that case the rapid optical variability has been explained as due to hot spots, or flares, or magnetic reconnection in the accretion disc. No clear evidence of large amplitude short-term variability in UV band has been reported for radio-quiet

NLSy1, with only small amplitude rapid variability observed for 1H 0707–495 (Robertson et al. 2015) and IRAS 13224–3809 (Buisson et al. 2018).

On the other hand, rapid optical variability has been observed in several blazars, the other class of γ -ray-emitting class of AGN with a relativistic jet pointed towards us (e.g., Miller et al. 1989; Carini et al. 1990; Heidt & Wagner 1996; Romero et al. 2002; Sagar et al. 2004). Such behaviour is usually observed during a flaring activity, but it may also be an observational bias due to the fact that intensive monitoring of blazars in optical is carried out mainly when the activity of the source is high. Similar events in UV are less common for blazars (e.g., Edelson 1992), although this can be related to the lack of dedicated monitoring programs in that energy range.

The detection of rapid variability in optical in blazars has been explained by invoking a shock moving down the jet (e.g., Marscher & Gear 1985), turbulent cells behind a shock in the jet (e.g., Marscher 2014), irregularities in the jet flow such as mini-jets (e.g., Giannios et al. 2009), or variations in the outflow parameters due to magnetic reconnection (e.g., Sironi et al. 2015; Christie et al. 2019). In all these scenarios it is important the Doppler boosting of the jet emission, which amplifies the amplitude and shorten the time-scale of the variation, and therefore the viewing angle of the emitting region has to be close to the observer’s line of sight (see e.g. Raiteri et al. 2017). In this context, the rapid and large variability episodes detected for these γ -ray-emitting NLSy1 clearly point to the presence of a relativistically beamed jet, closely aligned to our line of sight, similarly to blazars.

The detection of polarized emission has been considered the incontrovertible proof that the synchrotron emission dominates in the optical part of the spectrum of blazars (e.g., Itoh et al. 2016; Zhang 2019). Polarization as high as 10 per cent and 36 per cent has been detected in the γ -ray-emitting NLSy1 SBS 0846+513 (Maune et al. 2014) and PMN J0948+0022 (Itoh et al. 2013) accompanied by intraday variation in the photometric light curves. For 1H 0323+342, Itoh et al. (2014) reported an increase of the optical polarization degree from 0–1 per cent to 3 per cent during a high optical state. The lower polarization degree in this source may be due to the contamination from the thermal accretion disc emission also in the optical part of the spectrum. Significant polarization increase has been reported also for PKS 1502+036 in Angelakis et al. (2018). These results indicate the synchrotron origin from a compact region of the jet for the optical emission in these γ -ray-emitting NLSy1, at least during high activity states, confirming the similarity between these sources and blazars.

Taking into account the cosmological redshift of the source, we calculate the intrinsic variability time-scale as $\Delta T_{\text{rest}} = \Delta T / (1+z)$. This results in a minimum intrinsic variability time-scale of 3.2 ks for SBS 0846+513, 3.3 ks for PMN J0948+0022, 4.1 ks for PKS 2004–447, and 5.4 ks for 1H 0323+342, as reported in Table 3. Based on causality argument, it is possible to constrain the intrinsic size of the emitting region during these rapid variability events to be $R < c\delta\Delta T_{\text{rest}} = 1.6\text{--}4.9 \times 10^{15}$ cm for 1H 0323+342, 9.7×10^{14} cm for SBS 0846+513, $1.1\text{--}8.8 \times 10^{15}$ cm for PMN J0948+0022, and 1.4×10^{15} cm for PKS 2004–447 (assuming a typical Doppler factor $\delta = 10$). This suggests that the optical and UV emission during these

events is produced in compact regions within the jet. It is worth mentioning that the orbital period of the *Swift* satellite is 5700 s, and usually one exposure per orbit in each filter has been collected with UVOT and during the same portion of the orbit, limiting the minimum time between two exposures collected with the same filter to 5–6 ks. Therefore, the observed variability time-scale estimated here may be an upper limit to the effective time-scale of the variation and the intrinsic size of the emitting region may be smaller.

The minimum intrinsic variability estimated by the optical and UV observations for these NLSy1 can be also connected to the event horizon light crossing time of their supermassive black hole as $t_{lc} \sim r_g/c \sim GM_9/c^3 \sim 1.4 \times M_9$ h, where r_g is the gravitational radius, $M_9 = (M/10^9) M_\odot$ is the BH mass in solar masses, and c is the speed of light (e.g., Begelman et al. 2008). Assuming a BH mass of $10^9 M_\odot$, $t_{lc} \sim 1.4$ h. Comparing this value to the minimum intrinsic variability time-scale obtained for these sources provides an upper limit to their BH mass, which is a debated issue for γ -ray-emitting NLSy1 (see D’Ammando 2019, for a detailed discussion). In particular, we obtain an upper limit of $1.1 \times 10^9 M_\odot$ for 1H 0323+342, $6.4 \times 10^8 M_\odot$ for SBS 0846+513, $6.6 \times 10^8 M_\odot$ for PMN J0948+0022, and $8.2 \times 10^8 M_\odot$ for PKS 2004–447. A more dense short-term monitoring with more than one exposure per filter within the same orbit with *Swift* will be important to set tighter constraints to the minimum variability time-scale and therefore to the size of the emitting region and the BH mass of these objects.

4 SUMMARY

We have performed the first systematic analysis of single exposures of all optical and UV observations carried out by *Swift*–UVOT available up to 2019 April of six γ -ray-emitting NLSy1. Our main results are summarized below.

1. Significant ($> 3\sigma$) magnitude changes have been observed on hours time-scale for 1H 0323+342, SBS 0846+513, PMN J0948+0022, and PKS 2004–447 in 18 observations for a total of 34 events in different filters. After removing exposures affected by the ‘sss’ issue, there are 205 UVOT observations with multiple exposures at least in one filter in the same epoch. Rapid variability has been observed in ~ 9 per cent of the *Swift*–UVOT observations, with a percentage of events detected of ~ 3 per cent, ~ 1.5 per cent, and ~ 12 per cent for 1H 0323+342, SBS 0846+513, and PMN J0948+0022, respectively. Several other magnitude changes at a significance level $2 < \sigma < 3$ have been observed. These events provide unambiguous evidence about the relativistically beamed synchrotron emission in these γ -ray-emitting NLSy1, similar to what is observed in blazars. During these events a higher amplitude of variability has been observed in the optical bands with respect to the UV ones, in agreement with a dominant contribution of the synchrotron emission.

2. We have detected for the first time rapid variability in optical on time-scale of ~ 6 ks (~ 4.1 ks in the rest frame) in PKS 2004–447, and for the first time rapid variability in UV on time-scale of ~ 6 ks in 1H 0323+342 and PMN J0948+0022, corresponding to 5.4 and 3.4 ks in the rest frame, respectively.

3. For 1H 0323+342 and PMN J0948+0022, short-term

variability has been significantly detected in both optical and UV bands, at least one time for all six UVOT filters, except for the v filter in 1H 0323+342. A higher fractional flux change has been observed in PMN J0948+0022 with respect to 1H 0323+342. For PMN J0948+0022, the fractional flux change is higher in the optical filters than in the UV ones during these rapid variability events. For 1H 0323+342, the larger fractional flux changes have been observed in optical, where the jet emission should dominate, while a significant thermal emission from accretion disc is present in the UV part of the spectrum.

4. Notwithstanding SBS 0846+513 has shown the largest long-term variability amplitude in the optical and UV bands over the entire *Swift* monitoring, a change of magnitude has been significantly detected only in one observation. This is mainly due to the fact that the source is quite faint, therefore the uncertainties for the single exposures are relatively large, reducing the significance of the variations. On the contrary, for the brightest object in optical and UV, 1H 0323+342, although it did not show an extreme variability amplitude in the period studied, several episodes of short-term variability have been identified in both optical and UV bands.

5. For PKS 1502+036 and FBQS J1644+2619 no significant variability has been detected on hours time-scale. This can be related to the small number of *Swift* observations available for these sources but also to the faintness of PKS 1502+036 and the low activity of FBQS J1644+2619 in the period studied here.

6. Short variability time-scales can be used to extrapolate the size of the emitting region. The shortest variability time-scale observed in optical or UV for 1H 0323+342, SBS 0846+513, PMN J0948+0022, and PKS 2004–447 (assuming a Doppler factor $\delta = 10$) gives a lower limit on the size of emission region of $R < 1.6 \times 10^{15}$, 9.7×10^{14} , 1.1×10^{15} , and 1.4×10^{15} cm, respectively. This is an indication that the optical and UV emission during these events is produced in compact regions within the jet.

7. A remarkable variability has been observed for PMN J0948+0022 on 2009 June 23 with an increase from 1.1 to 0.4 mag going from v to $w2$ filter in ~ 1.6 h and a decrease at the initial level in a comparable time. The higher variability amplitude observed at lower frequencies suggests that the synchrotron emission is more contaminated by thermal emission from accretion disc at higher frequencies.

Swift–UVOT observations can be important for studying short-term variability in γ -ray-emitting NLSy1. From this first systematic analysis of six objects seems to emerge that an important factor for detecting rapid changes of magnitude is the average brightness of the target. In fact, the two sources for which the largest number of events have been detected are 1H 0323+342 and PMN J0948+0022, the brightest sources in the sample. This is directly related to the uncertainties obtained for single images, with large uncertainties reducing the significance of the detection, even if the change of magnitude is large. Such a kind of studies can be applied also to blazars, the other class of jetted AGN seen at a small angle to our line of sight. This will allow us to compare the properties of these two classes of γ -ray-emitting AGN in terms of rapid variability observed in optical and UV bands.

ACKNOWLEDGEMENTS

FD thanks the *Swift* team for making these observations possible, the duty scientists, and science planners. This research has made use of the XRT Data Analysis Software (XRT-DAS). This work made use of data supplied by the UK Swift Science Data Centre at the University of Leicester. This research has made use of data obtained through the High Energy Astrophysics Science Archive Research Center Online Service, provided by the NASA/Goddard Space Flight Center. This research has made use of the NASA/IPAC Extragalactic Database (NED), which is operated by the Jet Propulsion Laboratory, California Institute of Technology, under contract with the National Aeronautics and Space Administration. Part of this work is based on archival data, software or online services provided by the Space Science Data Center - ASI. FD thanks the anonymous referee for constructive comments and suggestions.

DATA AVAILABILITY

The data underlying this article are available in *Swift* Archive Download Portal at the UK *Swift* Science Data Centre (https://www.swift.ac.uk/swift_portal/).

REFERENCES

- Abdo, A. A., et al. 2009, *ApJ*, 707, L142
 Abdollahi, S., et al. 2020, *ApJS*, 247, 33
 Ajello, M., et al. 2020, *ApJ*, 892, 105
 Angelakis, E., Kiehlmann, S., Myserlis, I., Blinov, D., Eggen, J., Itoh, R., Marchili, N., Zensus, J. A. 2018, *A&A*, 618, A92
 Begelman M. C., Fabian A. C., Rees J. M. 2008, *MNRAS*, 384, L19
 Breeveld, A. A., et al. 2010, *MNRAS*, 406, 1687
 Buisson, D. J. K., et al. 2018, *MNRAS*, 475, 2306
 Cardelli, J. A., Clayton, G. C., Mathis, J. S. 1989, *ApJ*, 345, 245
 Carini, M. T., Miller, H. R., Goodrich, B. D. 1990, *AJ*, 100, 347
 Chiaberge, M., Ghisellini, G. 1999, *MNRAS*, 306, 551
 Christie, I. M., Petropoulou, M., Sironi, L., Giannios, D. 2019, *MNRAS*, 482, 65
 D’Ammando, F., et al. 2011, *A&A*, 529A, 145
 D’Ammando, F., et al. 2012, *MNRAS*, 426, 317
 D’Ammando, F., et al. 2013, *MNRAS*, 436, 191
 D’Ammando, F., Orienti, M., Larsson, J., Giroletti, M. 2015a, *MNRAS*, 452, 520
 D’Ammando, F., et al. 2015b, *MNRAS*, 446, 2456
 D’Ammando, F., Orienti, M., Finke, J., Larsson, J., Giroletti, M., Raiteri, C. 2016, *Galaxies*, 4, 11
 D’Ammando, F. 2019, *Galaxies*, 7, 87
 D’Ammando, F. 2020, *MNRAS*, 496, 2213
 Edelson, R. 1992, *ApJ*, 401, 516
 Eggen, J. R., Miller, H. R., Maune, J. D. 2013, *ApJ*, 773, 85
 Foschini, L., et al. 2015, *A&A*, 575A, 13
 Gehrels, N., et al. 2004, *ApJ*, 611, 1005
 Giannios, D., Uzdensky, D. A., Begelman, M. C. 2009, *MNRAS*, 395L, 29
 Grupe, D. 2004, *ApJ*, 127, 1799
 Itoh, R., et al. 2013, *ApJ*, 775, L26
 Itoh, R., et al. 2014, *PASJ*, 66, 108
 Itoh, R., et al. 2016, *ApJ*, 833, 77
 Järvelä, E., Berton, M., Ciroi, S., Congiu, E., Lähteenmäki, A., Di Mille, F. 2020, *A&A*, 636L, 12
 Jiang, L., Fan, X., Ivezić, Z., Richards, G. T., Schneider, D. P., Strauss, M. A., Kelly, B. 2007, *ApJ*, 656, 680
 Heidt, J., Wagner, S. J. 1996, *A&A*, 305, 42
 Kellermann, K. I., Condon, J. J., Kimball, A. E., Perley, R. A., Ivezić, Z. 2016, *ApJ*, 831, 168
 Klimek, E. S., Gaskell, C. M., Hedrick, C. H. 2004, *ApJ*, 609, 69
 Komossa, S., Voges, W., Xu, D., Mathur, S., Adorf, H., Lemson, G., Duschl, W. J., Grupe, D. 2006, *AJ*, 132, 531
 Liu, H., Wang, J., Mao, Y., Wei, J. 2010, *ApJ*, 715, L113
 Marscher, A. P., Gear, W. K. 1985, *ApJ*, 298, 114
 Marscher, A. P. 2014, *ApJ*, 780, 87
 Maune, J. D., Miller, H. R., Eggen, J. R. 2013, *ApJ*, 762, 124
 Maune, J. D., Eggen, J. R., Miller, H. R., Marshall, K., Readhead, A. C. S., Hovatta, T., King, O. 2014, *ApJ*, 794, 93
 Miller, H. R., Carini M. T., Goodrich B. D. 1989, *Nature*, 337, 627
 Miller, H. R., Ferrara, E. C., McFarland, J. P., Wilson, J. W., Daya, A. B., Fried, R. E. 2000, *New Astron. Rev.*, 44, 539
 Ojha, V., Krishna, G., Chand, H. 2019, *MNRAS*, 483, 3036
 Ojha, V., Chand, H., Krishna, G., Mishra, S., Chand, K. 2020, *MNRAS*, 493, 3642
 Orienti, M., D’Ammando, F., Larsson, J., Finke, J., Giroletti, M., Dallacasa, D., Isacsson, T., Stoby Hoglund, J. 2015, *MNRAS*, 453, 4037
 Paliya, V. S., & Stalin, C. S. 2016, *ApJ*, 820, 52
 Peterson, B. M., et al. 2000, *ApJ*, 542, 161
 Pogge, R. W. 2000, *New Astron. Rev.*, 44, 381
 Poole, T. S., et al. 2008, *MNRAS*, 383, 627
 Raiteri, C. M., et al. 2012, *A&A*, 545A, 48
 Raiteri, C. M., et al. 2017, *Nature*, 552, 374
 Rakshit, S., Stalin, C. S., Chand, H., Zhang, X.-G. 2017, *ApJS*, 229, 39
 Robertson, D. R. S., Gallo, L. C., Zoghbi, A., Fabian, A. C. 2015, *MNRAS*, 453, 3455
 Romero, G. E., Cellone, S. A., Combi, J. A., Andruchow, I. 2002, *A&A*, 390, 431
 Roming, P. W. A., et al. 2005, *Space Sci. Rev.*, 120, 95
 Sagar, R., Stalin, C. S., Gopal-Krishna, Wiita, P. J. 2004, *MNRAS*, 348, 176
 Schlafly, E. F. & Finkbeiner, D. P. 2011, *ApJ*, 737, 103
 Sironi, L., Petropoulou, M., Giannios, D. 2015, *MNRAS*, 450, 183
 Vanden Berk, D. E., et al. 2004, *ApJ*, 601, 692
 Zhang, H. 2019, *Galaxies*, 2019, 7, 85
 Zhou, H.-Y., Wang, T.-G., Yuan, W., Lu, H., Dong, X., Wang, J., Lu, Y. 2006, *ApJ*, 166, 128

APPENDIX A: SWIFT–UVOT SUMMED IMAGES RESULTS

For each epoch, we processed the images obtained by summing the exposures with the same filter in the same epoch with the task `uvotimsum` and then aperture photometry was performed with the task `uvotsource`. All images are aspect corrected to ensure that individual exposures are summed without offsets⁵. We extracted source counts from a circular region of 5 arcsec radius centred on the source, while background counts were derived from a circular region with 20 arcsec radius in a nearby source-free region. The observed magnitude obtained for the six sources are reported in Tables A1–A6. Values in italics refer to epochs in which multiple exposures with the same filter at the same epoch are available.

The average magnitudes in each UVOT filter for all sources are reported in Table A7. We have also calculated the long-term variability amplitude ($V_{\text{amp, LT}}$) for each filter, where $V_{\text{amp, LT}}$ is calculated as the ratio of maximum to minimum flux as $F_{\text{max}}/F_{\text{min}} = 2.581164^{\Delta \text{mag}_{\text{max}}}$, where $\Delta \text{mag}_{\text{max}} = \text{mag}_{\text{max}} - \text{mag}_{\text{min}}$, and mag_{max} and mag_{min} are the maximum and minimum magnitude observed, respectively, over the entire *Swift* monitoring period.

⁵ <https://www.swift.ac.uk/analysis/uvot/image.php>

Table A1. Observed magnitude of 1H 0323+324 obtained by *Swift*-UVOT.

Date (UT)	MJD	<i>v</i>	<i>b</i>	<i>u</i>	<i>w1</i>	<i>m2</i>	<i>w2</i>
2006-07-06	53922	15.54 ± 0.04	16.11 ± 0.07	15.13 ± 0.05	15.33 ± 0.05	15.63 ± 0.06	15.57 ± 0.07
2006-07-09	53925	—	16.04 ± 0.05	15.08 ± 0.05	15.30 ± 0.05	—	—
2007-07-20	54301	15.66 ± 0.04	16.23 ± 0.05	15.36 ± 0.05	15.61 ± 0.06	15.92 ± 0.06	15.82 ± 0.05
2007-11-04	54410	15.72 ± 0.05	16.36 ± 0.05	15.58 ± 0.06	15.86 ± 0.07	16.23 ± 0.08	16.09 ± 0.06
2007-11-11	54417	15.82 ± 0.05	16.41 ± 0.05	15.56 ± 0.05	15.79 ± 0.06	16.11 ± 0.08	15.98 ± 0.06
2007-11-25	54429	15.80 ± 0.05	16.34 ± 0.05	15.54 ± 0.05	15.84 ± 0.06	16.21 ± 0.07	16.06 ± 0.06
2007-12-01	54435	15.81 ± 0.05	16.36 ± 0.05	15.53 ± 0.05	15.84 ± 0.04	16.10 ± 0.07	16.01 ± 0.06
2007-12-06	54440	15.79 ± 0.04	16.33 ± 0.05	15.55 ± 0.05	15.79 ± 0.06	16.08 ± 0.06	16.04 ± 0.06
2007-12-15	54449	15.75 ± 0.05	16.40 ± 0.05	15.56 ± 0.05	15.76 ± 0.06	16.11 ± 0.07	15.95 ± 0.03
2007-12-23	54457	15.77 ± 0.05	16.39 ± 0.07	15.48 ± 0.05	15.74 ± 0.06	16.01 ± 0.07	15.88 ± 0.06
2007-12-28	54462	—	16.30 ± 0.05	15.46 ± 0.05	15.67 ± 0.06	—	15.80 ± 0.06
2008-01-04	54469	15.76 ± 0.05	16.31 ± 0.05	15.48 ± 0.05	15.70 ± 0.06	15.98 ± 0.07	15.89 ± 0.06
2008-01-14	54479	15.67 ± 0.05	16.24 ± 0.05	15.37 ± 0.05	15.58 ± 0.06	15.88 ± 0.07	15.71 ± 0.06
2008-11-16	54786	15.74 ± 0.04	16.31 ± 0.04	15.52 ± 0.05	15.83 ± 0.06	16.22 ± 0.06	16.07 ± 0.06
2009-07-24	55036	15.54 ± 0.05	16.15 ± 0.05	15.21 ± 0.05	15.49 ± 0.06	15.80 ± 0.06	15.66 ± 0.06
2009-07-27	55040	15.54 ± 0.05	16.18 ± 0.05	15.28 ± 0.05	15.55 ± 0.06	15.89 ± 0.07	15.75 ± 0.06
2009-07-30	55043	15.59 ± 0.05	16.15 ± 0.05	15.22 ± 0.05	15.52 ± 0.06	15.82 ± 0.07	15.72 ± 0.06
2009-08-02	55045	15.63 ± 0.05	16.17 ± 0.05	15.29 ± 0.07	15.51 ± 0.06	15.85 ± 0.07	15.70 ± 0.06
2009-08-05	55048	15.69 ± 0.05	16.17 ± 0.05	15.29 ± 0.05	15.54 ± 0.06	15.88 ± 0.07	15.79 ± 0.06
2009-08-08	55051	15.68 ± 0.05	16.22 ± 0.05	15.36 ± 0.05	15.66 ± 0.06	15.95 ± 0.07	15.89 ± 0.06
2010-10-28	55497	15.57 ± 0.05	16.08 ± 0.05	15.20 ± 0.05	15.48 ± 0.06	15.82 ± 0.07	15.73 ± 0.06
2010-10-29	55498	15.64 ± 0.05	16.13 ± 0.05	15.27 ± 0.05	15.59 ± 0.06	15.96 ± 0.07	15.94 ± 0.06
2010-10-30	55499	15.58 ± 0.05	16.08 ± 0.05	15.24 ± 0.05	15.51 ± 0.06	15.78 ± 0.07	15.71 ± 0.06
2010-10-31	55500	15.64 ± 0.04	—	—	—	—	15.74 ± 0.06
2010-11-02	55502	15.64 ± 0.05	16.17 ± 0.05	15.27 ± 0.05	15.53 ± 0.06	15.85 ± 0.06	15.75 ± 0.06
2010-11-03	55503	15.66 ± 0.04	—	—	—	—	15.77 ± 0.06
2010-11-04	55504	15.68 ± 0.04	—	—	—	—	15.78 ± 0.06
2010-11-05	55505	15.74 ± 0.04	—	—	—	—	15.85 ± 0.06
2010-11-06	55506	15.70 ± 0.04	—	—	—	—	15.90 ± 0.06
2010-11-07	55507	15.69 ± 0.05	16.14 ± 0.05	15.64 ± 0.05	15.64 ± 0.06	16.11 ± 0.07	15.96 ± 0.06
2010-11-08	55508	15.68 ± 0.04	—	—	—	—	15.83 ± 0.06
2010-11-09	55509	15.68 ± 0.04	—	—	—	—	15.75 ± 0.06
2010-11-10	55510	15.73 ± 0.04	—	—	—	—	15.85 ± 0.06
2010-11-11	55511	15.65 ± 0.04	—	—	—	—	15.65 ± 0.06
2010-11-12	55512	15.61 ± 0.05	16.16 ± 0.05	15.26 ± 0.05	15.52 ± 0.06	15.84 ± 0.07	15.65 ± 0.06
2010-11-13	55513	15.65 ± 0.04	—	—	—	—	15.65 ± 0.06
2010-11-14	55514	15.60 ± 0.04	—	—	—	—	15.66 ± 0.06
2010-11-15	55515	15.66 ± 0.04	—	—	—	—	15.66 ± 0.06
2010-11-16	55516	15.55 ± 0.04	—	—	—	—	15.65 ± 0.06
2010-11-17	55517	15.61 ± 0.05	16.09 ± 0.05	15.28 ± 0.05	15.50 ± 0.06	15.78 ± 0.07	15.67 ± 0.06
2010-11-18	55518	15.67 ± 0.04	—	—	—	—	15.65 ± 0.06
2010-11-19	55519	15.66 ± 0.04	—	—	—	—	15.84 ± 0.06
2010-11-23	55523	15.65 ± 0.05	16.11 ± 0.05	15.27 ± 0.05	15.48 ± 0.06	15.71 ± 0.07	15.63 ± 0.06
2010-11-24	55524	15.64 ± 0.05	16.18 ± 0.05	15.24 ± 0.05	15.46 ± 0.06	15.74 ± 0.07	15.62 ± 0.06
2010-11-25	55525	15.59 ± 0.05	16.09 ± 0.05	15.20 ± 0.05	15.37 ± 0.06	15.64 ± 0.06	15.54 ± 0.06
2010-11-26	55526	15.66 ± 0.04	—	—	—	—	15.64 ± 0.05
2010-11-27	55527	15.72 ± 0.04	—	—	—	—	15.98 ± 0.06
2010-11-28	55528	15.64 ± 0.04	—	—	—	—	15.64 ± 0.05
2010-11-29	55529	15.59 ± 0.04	—	—	—	—	15.59 ± 0.05
2010-11-30	55530	15.64 ± 0.05	16.11 ± 0.05	15.21 ± 0.05	15.46 ± 0.06	15.76 ± 0.06	15.70 ± 0.06
2011-07-06	55748	15.60 ± 0.06	16.15 ± 0.06	15.18 ± 0.06	15.44 ± 0.07	15.74 ± 0.07	15.60 ± 0.06
2011-07-07	55749	15.60 ± 0.06	16.06 ± 0.05	15.21 ± 0.05	15.35 ± 0.06	15.72 ± 0.07	15.58 ± 0.06
2011-09-04	55808	15.67 ± 0.06	16.17 ± 0.06	15.22 ± 0.05	15.48 ± 0.07	15.78 ± 0.08	15.64 ± 0.06
2011-10-03	55837	15.65 ± 0.06	16.15 ± 0.06	15.25 ± 0.06	15.44 ± 0.07	15.84 ± 0.08	15.69 ± 0.06
2011-10-07	55841	15.54 ± 0.06	16.11 ± 0.06	15.19 ± 0.06	15.39 ± 0.07	15.68 ± 0.07	15.59 ± 0.06
2011-11-05	55870	15.71 ± 0.07	16.14 ± 0.06	15.36 ± 0.06	15.62 ± 0.07	15.88 ± 0.06	15.73 ± 0.07
2011-12-04	55899	—	—	15.51 ± 0.07	15.69 ± 0.07	—	—
2011-12-07	55902	15.73 ± 0.09	16.40 ± 0.08	15.54 ± 0.08	15.76 ± 0.09	16.07 ± 0.06	15.99 ± 0.08
2011-12-28	55923	15.84 ± 0.06	16.39 ± 0.06	15.56 ± 0.06	15.78 ± 0.07	16.05 ± 0.07	15.96 ± 0.06
2012-01-02	55928	15.83 ± 0.09	—	—	15.75 ± 0.04	—	—

Date (UT)	MJD	<i>v</i>	<i>b</i>	<i>u</i>	<i>w1</i>	<i>m2</i>	<i>w2</i>
2012-01-30	55956	15.65 ± 0.07	16.26 ± 0.05	15.38 ± 0.05	15.66 ± 0.07	15.92 ± 0.09	15.97 ± 0.07
2012-03-03	55989	15.85 ± 0.06	16.48 ± 0.06	15.65 ± 0.06	15.90 ± 0.07	16.30 ± 0.08	16.22 ± 0.07
2013-01-13	56305	15.77 ± 0.05	16.33 ± 0.05	15.50 ± 0.05	15.75 ± 0.06	16.13 ± 0.07	15.99 ± 0.06
2013-01-14	56306	15.69 ± 0.05	16.38 ± 0.05	15.47 ± 0.05	15.73 ± 0.06	16.02 ± 0.07	15.94 ± 0.06
2013-01-15	56307	15.73 ± 0.05	16.32 ± 0.05	15.46 ± 0.05	15.72 ± 0.06	16.00 ± 0.06	15.93 ± 0.06
2013-02-15	56338	15.81 ± 0.05	16.33 ± 0.05	15.51 ± 0.05	15.78 ± 0.06	16.14 ± 0.07	16.07 ± 0.06
2013-02-15	56338	15.82 ± 0.05	16.38 ± 0.05	15.55 ± 0.05	15.83 ± 0.06	16.20 ± 0.07	16.09 ± 0.06
2013-03-02	56353	15.70 ± 0.07	16.09 ± 0.05	15.33 ± 0.05	15.67 ± 0.06	16.03 ± 0.08	15.87 ± 0.06
2013-03-05	56356	15.82 ± 0.06	16.38 ± 0.05	15.53 ± 0.05	15.76 ± 0.06	16.05 ± 0.08	15.91 ± 0.06
2013-07-12	56485	—	—	—	—	—	15.67 ± 0.05
2013-07-16	56489	15.49 ± 0.06	16.02 ± 0.06	15.16 ± 0.06	15.35 ± 0.06	15.70 ± 0.08	15.63 ± 0.05
2013-07-18	56491	15.54 ± 0.05	16.14 ± 0.05	15.25 ± 0.05	15.48 ± 0.06	15.82 ± 0.06	15.64 ± 0.06
2013-07-19	56492	15.51 ± 0.04	15.95 ± 0.05	15.13 ± 0.05	15.36 ± 0.06	15.69 ± 0.06	15.61 ± 0.06
2013-07-19	56492	15.53 ± 0.04	16.02 ± 0.05	15.18 ± 0.05	15.44 ± 0.06	15.77 ± 0.06	15.61 ± 0.06
2013-08-19	56523	15.67 ± 0.05	16.18 ± 0.05	15.26 ± 0.05	15.52 ± 0.06	15.75 ± 0.06	15.64 ± 0.06
2013-08-20	56524	15.59 ± 0.05	16.13 ± 0.05	15.26 ± 0.05	15.41 ± 0.06	15.73 ± 0.06	15.62 ± 0.06
2013-08-21	56525	15.69 ± 0.05	16.11 ± 0.05	15.24 ± 0.05	15.46 ± 0.06	15.72 ± 0.06	15.61 ± 0.06
2013-08-30	56534	15.52 ± 0.04	16.06 ± 0.05	15.16 ± 0.05	15.47 ± 0.06	15.82 ± 0.07	15.67 ± 0.06
2013-09-06	56541	15.58 ± 0.05	16.04 ± 0.05	15.12 ± 0.05	15.34 ± 0.06	15.64 ± 0.07	15.54 ± 0.06
2013-09-13	56548	15.47 ± 0.05	15.97 ± 0.05	15.08 ± 0.05	15.24 ± 0.06	15.51 ± 0.07	15.41 ± 0.06
2013-09-20	56555	15.46 ± 0.05	15.96 ± 0.05	15.03 ± 0.05	15.32 ± 0.06	15.69 ± 0.07	15.53 ± 0.06
2013-09-27	56562	15.51 ± 0.06	16.05 ± 0.05	15.14 ± 0.05	15.36 ± 0.07	15.64 ± 0.07	15.56 ± 0.06
2013-10-02	56567	15.58 ± 0.06	16.08 ± 0.06	15.14 ± 0.06	15.47 ± 0.07	15.66 ± 0.08	15.54 ± 0.07
2014-12-10	57001	15.50 ± 0.05	16.05 ± 0.05	15.16 ± 0.05	15.41 ± 0.06	15.75 ± 0.06	15.68 ± 0.06
2014-12-12	57003	15.61 ± 0.05	16.16 ± 0.05	15.23 ± 0.05	15.50 ± 0.06	15.92 ± 0.07	15.86 ± 0.06
2015-08-02	57236	15.68 ± 0.05	16.21 ± 0.05	15.40 ± 0.05	15.59 ± 0.06	15.93 ± 0.07	15.96 ± 0.06
2015-08-05	57239	15.68 ± 0.05	16.26 ± 0.05	15.40 ± 0.05	15.62 ± 0.06	16.12 ± 0.07	16.00 ± 0.06
2015-08-11	57245	15.69 ± 0.05	16.22 ± 0.05	15.28 ± 0.05	15.52 ± 0.06	15.82 ± 0.07	15.70 ± 0.06
2015-08-17	57251	15.74 ± 0.06	16.24 ± 0.06	15.38 ± 0.06	15.63 ± 0.07	16.01 ± 0.08	15.97 ± 0.07
2015-08-20	57254	15.70 ± 0.06	16.21 ± 0.05	15.39 ± 0.05	15.56 ± 0.06	15.94 ± 0.08	15.83 ± 0.06
2015-08-23	57257	15.66 ± 0.05	16.25 ± 0.05	15.40 ± 0.05	15.66 ± 0.06	15.95 ± 0.07	15.94 ± 0.06
2015-08-26	57260	15.65 ± 0.05	16.23 ± 0.05	15.35 ± 0.05	15.58 ± 0.06	15.93 ± 0.07	15.90 ± 0.06
2015-08-29	57263	15.68 ± 0.05	16.28 ± 0.05	15.44 ± 0.05	15.65 ± 0.07	16.03 ± 0.07	15.98 ± 0.06
2015-09-10	57275	15.72 ± 0.06	16.25 ± 0.05	15.38 ± 0.05	15.61 ± 0.07	15.91 ± 0.10	15.85 ± 0.06
2015-09-17	57282	15.61 ± 0.06	16.15 ± 0.06	15.30 ± 0.06	15.51 ± 0.07	15.79 ± 0.08	15.71 ± 0.06
2015-09-24	57289	15.68 ± 0.07	16.14 ± 0.06	15.24 ± 0.05	15.39 ± 0.06	15.65 ± 0.08	15.56 ± 0.07
2015-09-29	57294	15.59 ± 0.05	16.07 ± 0.05	15.12 ± 0.05	15.32 ± 0.06	15.61 ± 0.07	15.47 ± 0.06
2015-10-08	57303	15.54 ± 0.05	16.04 ± 0.05	15.11 ± 0.05	15.19 ± 0.06	15.58 ± 0.07	15.43 ± 0.06
2015-10-15	57310	15.52 ± 0.05	16.06 ± 0.05	15.09 ± 0.05	15.34 ± 0.07	15.68 ± 0.17	15.60 ± 0.06
2015-10-22	57317	15.56 ± 0.05	16.07 ± 0.05	15.11 ± 0.05	15.35 ± 0.06	15.67 ± 0.07	15.54 ± 0.06
2015-10-31	57326	15.55 ± 0.05	16.07 ± 0.05	15.22 ± 0.05	15.49 ± 0.07	15.83 ± 0.06	15.78 ± 0.06
2015-11-05	57331	15.64 ± 0.05	16.12 ± 0.05	15.27 ± 0.05	15.54 ± 0.06	15.91 ± 0.07	15.85 ± 0.06
2015-11-12	57338	15.57 ± 0.05	16.12 ± 0.05	15.16 ± 0.05	15.45 ± 0.06	15.78 ± 0.07	15.67 ± 0.06
2015-11-19	57345	15.66 ± 0.06	16.13 ± 0.05	15.30 ± 0.05	15.46 ± 0.07	15.92 ± 0.07	15.78 ± 0.06
2015-11-26	57352	15.58 ± 0.05	16.17 ± 0.05	15.31 ± 0.05	15.49 ± 0.07	15.82 ± 0.07	15.77 ± 0.06
2015-12-03	57359	15.66 ± 0.08	16.23 ± 0.07	15.26 ± 0.07	15.57 ± 0.09	15.89 ± 0.10	15.79 ± 0.08
2015-12-08	57364	15.57 ± 0.09	16.14 ± 0.06	15.32 ± 0.05	15.53 ± 0.06	15.88 ± 0.13	15.82 ± 0.09
2015-12-10	57366	—	—	15.40 ± 0.14	15.49 ± 0.07	—	—
2015-12-15	57371	15.67 ± 0.07	16.22 ± 0.06	15.33 ± 0.06	15.55 ± 0.08	16.01 ± 0.12	15.74 ± 0.06
2015-12-17	57373	—	16.18 ± 0.05	15.37 ± 0.06	15.53 ± 0.07	—	15.74 ± 0.08
2015-12-24	57380	15.67 ± 0.05	16.17 ± 0.05	15.34 ± 0.05	15.51 ± 0.07	15.88 ± 0.07	15.81 ± 0.06
2018-07-05	58304	—	—	15.47 ± 0.05	—	—	—
2018-07-12	58311	—	—	—	15.65 ± 0.06	—	—
2018-07-19	58318	—	—	—	—	16.17 ± 0.07	—
2018-07-26	58325	—	—	—	—	—	15.96 ± 0.06
2018-08-02	58332	—	—	15.69 ± 0.05	—	—	—
2018-08-09	58339	—	—	—	15.59 ± 0.06	—	—

Date (UT)	MJD	<i>v</i>	<i>b</i>	<i>u</i>	<i>w1</i>	<i>m2</i>	<i>w2</i>
2018-08-16	58346	—	—	—	—	15.94 ± 0.07	—
2018-08-23	58353	—	—	—	—	—	15.77 ± 0.06
2018-08-30	58360	—	—	15.52 ± 0.05	—	—	—
2018-09-06	58367	—	—	—	15.65 ± 0.06	—	—
2018-09-13	58374	—	—	—	—	15.94 ± 0.07	—
2018-09-20	58381	—	—	—	—	—	15.89 ± 0.06
2018-09-27	58388	—	—	15.58 ± 0.05	—	—	—
2018-10-04	58395	—	—	—	15.69 ± 0.06	—	—
2018-10-11	58402	—	—	—	—	16.05 ± 0.07	—
2018-10-18	58409	—	—	—	—	—	15.91 ± 0.06
2018-10-25	58416	—	—	15.64 ± 0.05	—	—	—
2018-11-01	58423	—	—	—	15.63 ± 0.06	—	—
2018-11-08	58430	—	—	—	—	16.08 ± 0.07	—
2018-11-15	58437	—	—	—	—	—	15.98 ± 0.06
2018-11-22	58444	—	—	15.57 ± 0.05	—	—	—
2018-11-29	58451	—	—	—	15.70 ± 0.06	—	—
2018-12-06	58458	—	—	—	—	16.11 ± 0.07	—
2018-12-13	58455	—	—	—	—	—	16.03 ± 0.06

Table A2. Observed magnitude of SBS0846+513 obtained by *Swift*-UVOT.

Date (UT)	MJD	<i>v</i>	<i>b</i>	<i>u</i>	<i>w1</i>	<i>m2</i>	<i>w2</i>
2011-08-30	55803	—	—	—	19.32 ± 0.08	—	—
2011-09-15	55819	18.78 ± 0.23	19.67 ± 0.20	19.09 ± 0.16	19.21 ± 0.15	19.39 ± 0.16	19.35 ± 0.12
2011-12-20	55915	> 18.64	> 19.81	> 19.44	19.86 ± 0.22	19.53 ± 0.39	19.84 ± 0.29
2011-12-27	55922	—	20.13 ± 0.42	19.85 ± 0.43	19.88 ± 0.35	19.58 ± 0.23	20.06 ± 0.31
2011-12-28	55923	> 18.91	> 19.92	19.12 ± 0.31	19.81 ± 0.16	19.84 ± 0.40	20.11 ± 0.34
2012-01-03	55929	—	—	—	—	—	20.32 ± 0.39
2012-05-27	56074	16.51 ± 0.08	17.22 ± 0.07	16.79 ± 0.08	17.35 ± 0.10	17.28 ± 0.10	17.58 ± 0.09
2012-06-06	56084	17.60 ± 0.13	18.30 ± 0.13	17.91 ± 0.13	18.34 ± 0.14	18.40 ± 0.13	18.70 ± 0.12
2012-10-30	56230	18.99 ± 0.36	> 20.08	19.77 ± 0.38	19.88 ± 0.35	19.69 ± 0.12	19.85 ± 0.24
2012-11-30	56261	> 18.50	19.69 ± 0.36	> 19.50	19.48 ± 0.31	19.16 ± 0.26	19.86 ± 0.12
2012-12-30	56291	18.67 ± 0.27	19.95 ± 0.35	> 19.71	19.62 ± 0.12	19.95 ± 0.33	20.10 ± 0.26
2013-01-30	56322	19.10 ± 0.40	19.76 ± 0.31	> 19.68	19.98 ± 0.39	19.88 ± 0.14	19.90 ± 0.24
2013-04-22	56404	16.14 ± 0.04	16.82 ± 0.06	16.39 ± 0.06	16.75 ± 0.07	16.60 ± 0.09	17.05 ± 0.07
2013-04-27	56409	17.72 ± 0.11	18.48 ± 0.11	18.04 ± 0.12	18.51 ± 0.14	18.63 ± 0.13	18.77 ± 0.11
2019-01-02	58485	18.72 ± 0.26	20.10 ± 0.35	19.39 ± 0.27	19.49 ± 0.29	19.30 ± 0.25	19.19 ± 0.18
2019-01-09	58492	19.10 ± 0.41	20.23 ± 0.35	19.51 ± 0.26	19.37 ± 0.24	> 20.12	19.60 ± 0.25
2019-01-16	58499	18.78 ± 0.25	19.43 ± 0.20	19.31 ± 0.24	20.09 ± 0.40	19.31 ± 0.24	19.52 ± 0.18
2019-01-23	58506	18.83 ± 0.25	19.38 ± 0.19	19.18 ± 0.21	19.62 ± 0.29	19.09 ± 0.19	19.33 ± 0.17
2019-01-30	58513	18.68 ± 0.47	19.46 ± 0.24	19.33 ± 0.26	19.36 ± 0.27	> 19.15	> 19.57
2019-02-04	58518	18.84 ± 0.30	19.66 ± 0.27	19.43 ± 0.20	19.66 ± 0.35	19.13 ± 0.22	19.56 ± 0.23
2019-02-06	58520	19.08 ± 0.30	19.93 ± 0.27	19.48 ± 0.26	19.52 ± 0.30	19.64 ± 0.25	19.46 ± 0.18
2019-02-13	58527	19.01 ± 0.28	19.74 ± 0.23	19.52 ± 0.26	19.18 ± 0.21	19.09 ± 0.18	19.23 ± 0.16
2019-02-20	58534	—	20.07 ± 0.29	19.51 ± 0.26	19.20 ± 0.22	—	19.29 ± 0.19
2019-02-27	58541	18.92 ± 0.27	19.75 ± 0.24	19.62 ± 0.29	19.47 ± 0.26	19.12 ± 0.20	19.40 ± 0.18
2019-03-06	58548	19.30 ± 0.37	20.00 ± 0.30	19.36 ± 0.24	19.39 ± 0.26	19.11 ± 0.21	19.30 ± 0.17
2019-03-13	58555	18.64 ± 0.22	19.73 ± 0.24	18.84 ± 0.17	19.29 ± 0.25	19.25 ± 0.21	19.11 ± 0.15
2019-03-20	58562	18.56 ± 0.19	19.41 ± 0.19	19.04 ± 0.20	19.02 ± 0.21	18.89 ± 0.17	19.15 ± 0.15
2019-03-27	58569	19.01 ± 0.30	19.79 ± 0.26	19.34 ± 0.25	18.86 ± 0.20	19.09 ± 0.19	19.10 ± 0.16
2019-04-03	58576	> 19.28	19.77 ± 0.27	19.56 ± 0.34	18.97 ± 0.25	18.97 ± 0.19	19.10 ± 0.16
2019-04-10	58583	18.95 ± 0.28	19.68 ± 0.23	19.77 ± 0.33	19.10 ± 0.29	19.04 ± 0.19	19.40 ± 0.18
2019-04-17	58590	18.95 ± 0.28	19.86 ± 0.25	19.50 ± 0.27	19.20 ± 0.23	18.85 ± 0.17	19.18 ± 0.16
2019-04-24	58597	18.90 ± 0.27	19.90 ± 0.29	19.31 ± 0.25	19.38 ± 0.27	19.55 ± 0.24	19.53 ± 0.19

Table A3. Observed magnitude of PMN J0948+0022 obtained by *Swift*-UVOT.

Date (UT)	MJD	<i>v</i>	<i>b</i>	<i>u</i>	<i>w1</i>	<i>m2</i>	<i>w2</i>
2008-12-05	54805	18.08 ± 0.13	18.51 ± 0.10	17.72 ± 0.08	17.48 ± 0.06	17.64 ± 0.09	17.62 ± 0.11
2009-03-26	54916	17.56 ± 0.07	17.90 ± 0.07	17.05 ± 0.06	17.06 ± 0.07	17.05 ± 0.08	17.05 ± 0.06
2009-04-15	54936	17.82 ± 0.11	18.22 ± 0.08	17.19 ± 0.07	17.07 ± 0.07	17.02 ± 0.08	17.13 ± 0.10
2009-05-05	54956	17.23 ± 0.07	17.74 ± 0.07	16.80 ± 0.06	16.86 ± 0.07	16.94 ± 0.07	16.95 ± 0.06
2009-05-10	54961	17.87 ± 0.11	18.13 ± 0.08	17.23 ± 0.07	17.10 ± 0.07	17.18 ± 0.08	17.19 ± 0.16
2009-05-15	54966	18.26 ± 0.26	18.31 ± 0.16	17.62 ± 0.14	17.34 ± 0.10	17.50 ± 0.13	17.64 ± 0.10
2009-05-25	54976	17.78 ± 0.12	18.29 ± 0.09	17.37 ± 0.07	17.21 ± 0.07	17.20 ± 0.08	17.29 ± 0.06
2009-06-04	54986	17.62 ± 0.10	18.01 ± 0.08	17.08 ± 0.07	17.05 ± 0.07	17.15 ± 0.08	17.17 ± 0.06
2009-06-14	54996	17.42 ± 0.10	17.88 ± 0.08	17.08 ± 0.07	17.01 ± 0.07	17.11 ± 0.08	17.17 ± 0.07
2009-06-23	55005	17.77 ± 0.10	17.97 ± 0.07	17.26 ± 0.06	17.14 ± 0.07	17.27 ± 0.07	17.22 ± 0.06
2009-06-24	55006	18.19 ± 0.16	18.48 ± 0.11	17.69 ± 0.09	17.35 ± 0.08	17.43 ± 0.08	17.46 ± 0.07
2009-07-03	55015	18.36 ± 0.22	18.50 ± 0.13	17.57 ± 0.09	17.34 ± 0.08	17.54 ± 0.09	17.40 ± 0.07
2010-07-03	55380	17.58 ± 0.19	18.20 ± 0.15	17.21 ± 0.10	17.08 ± 0.10	17.30 ± 0.12	17.20 ± 0.08
2011-04-29	55680	—	—	17.27 ± 0.05	—	—	—
2011-05-15	55696	18.15 ± 0.13	18.44 ± 0.10	17.66 ± 0.08	17.42 ± 0.08	17.40 ± 0.08	17.43 ± 0.07
2011-05-28	55709	17.95 ± 0.14	18.30 ± 0.10	17.46 ± 0.08	17.28 ± 0.08	17.31 ± 0.09	17.31 ± 0.07
2011-06-04	55716	—	—	17.08 ± 0.05	—	—	—
2011-06-14	55726	17.83 ± 0.11	18.21 ± 0.09	17.31 ± 0.07	17.30 ± 0.08	17.33 ± 0.05	17.25 ± 0.06
2011-07-02	55744	—	—	17.64 ± 0.06	—	—	—
2011-10-09	55843	—	—	16.74 ± 0.07	—	—	—
2011-10-12	55846	—	—	17.18 ± 0.05	—	—	—
2011-11-05	55870	—	—	17.19 ± 0.05	—	—	—
2011-12-08	55903	—	—	17.63 ± 0.06	—	—	—
2012-01-02	55928	—	—	17.56 ± 0.05	—	—	—
2012-01-05	55931	—	—	17.63 ± 0.07	—	—	—
2012-01-31	55957	—	—	17.55 ± 0.06	—	—	—
2012-02-27	55984	—	—	17.58 ± 0.05	—	—	—
2012-03-26	56012	—	—	17.62 ± 0.05	—	—	—
2012-03-30	56016	—	—	17.09 ± 0.05	—	—	—
2012-04-23	56040	—	—	17.36 ± 0.06	—	—	—
2012-04-28	56045	—	—	17.82 ± 0.05	—	—	—
2012-05-21	56068	—	—	17.22 ± 0.06	—	—	—
2012-06-18	56096	—	—	17.37 ± 0.05	—	—	—
2012-06-30	56108	—	—	17.56 ± 0.07	—	—	—
2012-11-05	56236	—	—	17.46 ± 0.05	—	—	—
2012-12-03	56264	—	—	17.42 ± 0.05	—	—	—
2012-12-25	56286	18.04 ± 0.17	18.26 ± 0.11	17.30 ± 0.09	17.24 ± 0.07	17.26 ± 0.11	17.39 ± 0.08
2012-12-30	56291	16.01 ± 0.10	16.59 ± 0.09	15.88 ± 0.08	16.18 ± 0.08	15.84 ± 0.11	16.02 ± 0.09
2013-01-03	56295	17.52 ± 0.10	17.93 ± 0.08	17.17 ± 0.07	17.03 ± 0.08	17.11 ± 0.08	17.06 ± 0.07
2013-01-11	56303	17.70 ± 0.12	17.87 ± 0.08	17.02 ± 0.07	16.91 ± 0.08	16.96 ± 0.08	17.07 ± 0.07
2013-01-17	56309	17.47 ± 0.09	17.79 ± 0.07	16.99 ± 0.07	16.96 ± 0.08	16.96 ± 0.08	16.97 ± 0.07
2016-04-21	57499	—	—	17.24 ± 0.19	—	—	—
2016-06-08	57547	17.86 ± 0.17	18.42 ± 0.13	17.46 ± 0.10	17.27 ± 0.10	17.36 ± 0.14	17.34 ± 0.08
2016-06-13	57552	17.59 ± 0.15	18.47 ± 0.15	17.20 ± 0.09	17.09 ± 0.10	17.28 ± 0.11	17.25 ± 0.08
2016-06-24	57563	18.61 ± 0.37	18.50 ± 0.18	17.70 ± 0.14	17.28 ± 0.11	17.56 ± 0.13	17.45 ± 0.09

Table A4. Observed magnitude of PKS 1502+036 obtained by *Swift*–UVOT.

Date (UT)	MJD	<i>v</i>	<i>b</i>	<i>u</i>	<i>w1</i>	<i>m2</i>	<i>w2</i>
2009-07-25	55037	18.98 ± 0.22	19.47 ± 0.17	18.60 ± 0.13	18.46 ± 0.11	18.37 ± 0.11	18.38 ± 0.08
2012-04-25	56042	18.62 ± 0.35	19.76 ± 0.40	19.11 ± 0.33	18.89 ± 0.24	18.81 ± 0.09	18.49 ± 0.15
2012-05-25	56072	18.67 ± 0.35	19.59 ± 0.32	18.59 ± 0.06	18.22 ± 0.16	18.45 ± 0.19	18.18 ± 0.12
2012-06-25	56103	18.74 ± 0.39	19.23 ± 0.33	18.72 ± 0.31	18.32 ± 0.07	18.16 ± 0.18	18.51 ± 0.16
2012-08-07	56146	19.46 ± 0.37	20.09 ± 0.30	18.95 ± 0.18	18.61 ± 0.13	18.51 ± 0.12	18.50 ± 0.09
2012-08-08	56147	> 18.81	19.15 ± 0.33	18.82 ± 0.36	19.12 ± 0.34	18.40 ± 0.20	18.45 ± 0.15
2015-12-22	57378	18.26 ± 0.22	18.52 ± 0.18	17.84 ± 0.11	17.72 ± 0.10	17.79 ± 0.10	17.93 ± 0.11
2015-12-25	57381	> 18.37	18.98 ± 0.29	18.49 ± 0.25	18.39 ± 0.21	18.01 ± 0.16	18.36 ± 0.10
2016-01-01	57388	> 18.12	> 19.25	> 20.20	18.14 ± 0.19	18.25 ± 0.19	18.35 ± 0.16
2016-01-08	57395	> 18.55	19.07 ± 0.26	18.53 ± 0.22	18.09 ± 0.09	18.18 ± 0.18	18.18 ± 0.13
2016-01-14	57401	> 18.28	18.89 ± 0.25	18.20 ± 0.21	18.01 ± 0.08	18.23 ± 0.20	18.08 ± 0.08
2016-01-22	57409	> 17.82	> 18.89	18.52 ± 0.36	18.05 ± 0.25	17.90 ± 0.22	18.06 ± 0.12
2016-06-06	57545	—	—	—	—	—	18.33 ± 0.12
2016-06-14	57553	> 18.71	19.38 ± 0.30	18.75 ± 0.26	18.56 ± 0.23	18.66 ± 0.23	18.49 ± 0.10
2016-06-24	57563	18.60 ± 0.30	19.52 ± 0.34	19.23 ± 0.39	18.58 ± 0.11	18.74 ± 0.23	18.54 ± 0.15
2017-02-12	57796	—	—	18.63 ± 0.07	—	—	—

Table A5. Observed magnitude of FBQS J1644+2619 obtained by *Swift*–UVOT.

Date (UT)	MJD	<i>v</i>	<i>b</i>	<i>u</i>	<i>w1</i>	<i>m2</i>	<i>w2</i>
2011-12-26	55921	17.64 ± 0.22	18.18 ± 0.16	16.80 ± 0.10	16.97 ± 0.11	16.88 ± 0.12	16.92 ± 0.07
2015-04-08	57120	—	—	17.32 ± 0.07	—	—	—
2015-04-09	57121	17.44 ± 0.16	18.02 ± 0.13	17.31 ± 0.12	17.23 ± 0.13	17.35 ± 0.13	17.26 ± 0.07
2015-05-05	57147	17.88 ± 0.28	18.26 ± 0.19	17.24 ± 0.15	17.45 ± 0.08	17.52 ± 0.18	17.49 ± 0.14
2015-06-05	57178	—	—	—	17.36 ± 0.08	17.52 ± 0.12	—
2015-07-05	57208	—	—	17.17 ± 0.05	—	—	—
2015-08-05	57239	17.55 ± 0.15	17.95 ± 0.12	16.90 ± 0.09	17.04 ± 0.07	17.07 ± 0.11	16.98 ± 0.09
2015-09-05	57270	17.77 ± 0.18	18.06 ± 0.16	17.20 ± 0.13	17.08 ± 0.12	17.13 ± 0.09	17.21 ± 0.10
2017-02-27	57811	17.52 ± 0.11	17.91 ± 0.08	16.93 ± 0.07	16.92 ± 0.08	17.05 ± 0.09	17.03 ± 0.07
2017-03-07	57819	17.36 ± 0.10	18.00 ± 0.08	17.04 ± 0.07	17.10 ± 0.09	17.29 ± 0.09	17.13 ± 0.08
2018-01-18	58136	—	—	17.30 ± 0.05	—	—	—

Table A6. Observed magnitude of PKS 2004–447 obtained by *Swift*–UVOT.

Date (UT)	MJD	<i>v</i>	<i>b</i>	<i>u</i>	<i>w1</i>	<i>m2</i>	<i>w2</i>
2011-05-15	55696	18.71 ± 0.11	19.93 ± 0.19	19.08 ± 0.13	19.86 ± 0.21	20.26 ± 0.28	20.49 ± 0.26
2011-07-14	55756	19.35 ± 0.21	19.83 ± 0.16	19.27 ± 0.13	19.92 ± 0.24	20.17 ± 0.30	20.26 ± 0.26
2011-07-19	55761	18.67 ± 0.31	—	> 18.96	> 19.40	> 19.29	> 19.63
2011-07-23	55765	19.63 ± 0.45	20.58 ± 0.47	19.27 ± 0.22	19.60 ± 0.32	> 20.18	19.84 ± 0.33
2011-08-10	55783	—	—	—	19.57 ± 0.24	—	—
2011-08-13	55786	18.69 ± 0.33	19.56 ± 0.31	19.32 ± 0.34	19.68 ± 0.37	20.05 ± 0.26	20.31 ± 0.35
2011-09-05	55809	18.64 ± 0.47	19.58 ± 0.51	18.85 ± 0.40	19.20 ± 0.42	> 19.55	20.17 ± 0.30
2011-09-17	55821	18.31 ± 0.09	19.00 ± 0.08	18.62 ± 0.08	19.27 ± 0.14	20.01 ± 0.24	19.93 ± 0.20
2011-11-15	55880	18.95 ± 0.19	19.66 ± 0.15	19.51 ± 0.19	19.94 ± 0.26	20.34 ± 0.33	20.66 ± 0.37
2012-03-14	56000	18.92 ± 0.17	19.55 ± 0.15	19.40 ± 0.18	20.06 ± 0.27	20.22 ± 0.28	20.10 ± 0.22
2012-07-03	56111	—	—	—	19.57 ± 0.10	—	—
2012-07-22	56130	—	—	—	—	19.98 ± 0.17	—
2012-09-12	56182	18.55 ± 0.26	19.75 ± 0.32	18.90 ± 0.22	19.61 ± 0.34	19.83 ± 0.13	19.99 ± 0.26
2012-09-22	56192	19.31 ± 0.51	19.53 ± 0.27	18.83 ± 0.22	19.43 ± 0.35	19.82 ± 0.33	20.13 ± 0.29
2012-09-30	56200	—	—	19.06 ± 0.07	—	—	—
2013-07-07	56480	—	—	18.84 ± 0.05	—	—	19.90 ± 0.23
2013-07-14	56487	—	—	18.65 ± 0.07	19.47 ± 0.08	—	—
2013-09-27	56562	—	—	—	19.02 ± 0.08	19.21 ± 0.14	—
2013-10-13	56578	—	—	—	—	19.67 ± 0.12	—
2013-10-20	56585	—	—	—	—	19.67 ± 0.11	—
2013-10-27	56592	—	—	18.73 ± 0.10	—	—	19.80 ± 0.19
2013-10-29	56594	—	—	—	—	19.75 ± 0.19	—
2013-11-03	56599	—	—	—	19.30 ± 0.11	—	—
2013-11-19	56615	—	—	—	19.05 ± 0.10	—	—
2013-11-20	56620	—	—	18.52 ± 0.03	—	—	—
2014-03-14	56730	—	—	—	19.62 ± 0.11	19.75 ± 0.43	—
2014-03-16	56732	—	—	18.90 ± 0.06	—	—	—
2016-04-27	57505	—	—	—	—	—	19.66 ± 0.13
2016-05-01	57509	—	—	—	—	19.18 ± 0.14	19.82 ± 0.14
2016-05-10	57518	—	—	—	—	19.51 ± 0.16	—
2016-10-24	57685	—	—	—	—	—	19.65 ± 0.16

Table A7. Average magnitude of the γ -ray-emitting NLSy1 in the UVOT filters based on summed images obtained by summing the single exposures collected at each epoch.

Source name	<i>v</i>	<i>b</i>	<i>u</i>	<i>w1</i>	<i>m2</i>	<i>w2</i>
1H 0323+342	15.65	16.19	15.34	15.56	15.89	15.78
SBS 0846+513	18.58	19.48	19.07	19.24	19.09	19.33
PMN J0948+0022	17.76	18.12	17.32	17.13	17.20	17.21
PKS 1502+036	18.76	19.30	18.64	18.37	18.32	18.32
FBQS J1644+2619	17.59	18.05	17.12	17.14	17.23	17.15
PKS 2004–447	18.88	19.70	18.97	19.54	19.84	20.05

Table A8. Long-term variability amplitude of the γ -ray-emitting NLSy1 in the UVOT filters based on summed images obtained by summing the single exposures collected at each epoch.

Source name	<i>v</i>	<i>b</i>	<i>u</i>	<i>w1</i>	<i>m2</i>	<i>w2</i>
1H 0323+342	1.45	1.64	1.89	1.96	2.12	2.16
SBS 0846+513	18.36	23.12	24.21	21.68	21.88	20.32
PMN J0948+0022	10.96	5.86	5.97	3.31	5.25	4.45
PKS 1502+036	3.02	4.25	3.60	3.63	2.56	1.75
FBQS J1644+2619	1.61	1.38	1.61	1.63	1.80	1.69
PKS 2004–447	3.37	4.29	2.49	2.61	2.91	2.54

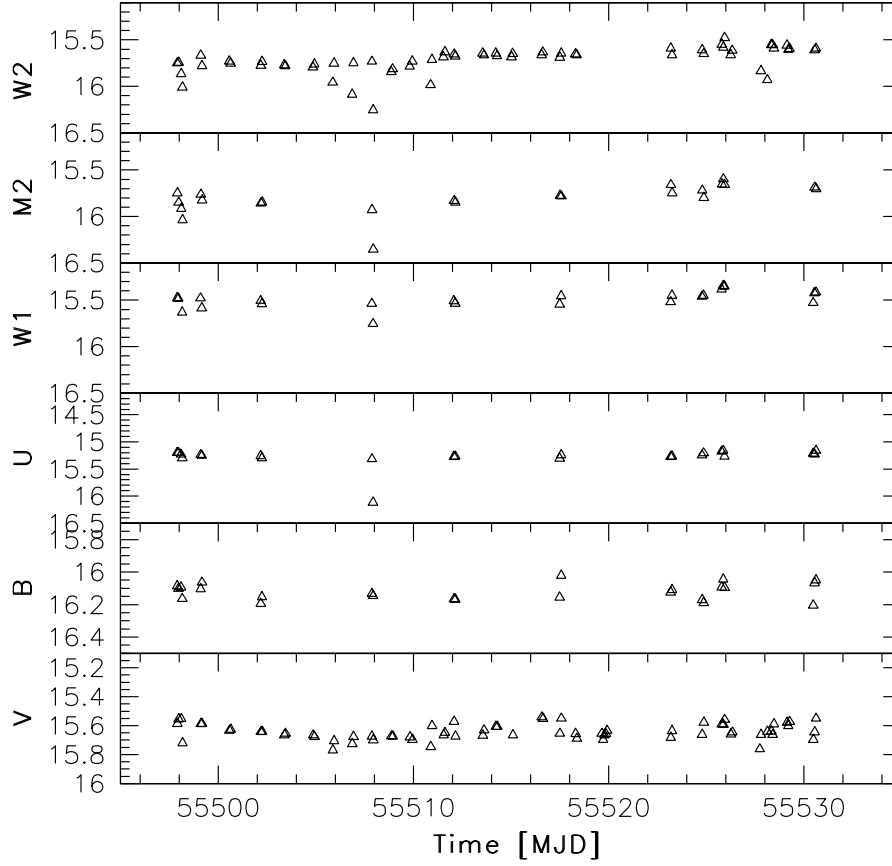


Figure A1. Light curve of 1H 0323+342 in the UVOT filters for the period 2010 October 28 (MJD 55497)–November 30 (MJD 55530) considering single exposures. Errors are quite small (0.04–0.06 mag) and are not shown in the plot.